Science of the Total Environment 728 (2020) 138848

Contents lists available at ScienceDirect

Science of the Total Environment

journal homepage: www.elsevier.com/locate/scitotenv

Hydrogeochemical, isotopic and geophysical characterization of saline lake systems in semiarid regions: The Salada de Chiprana Lake, Northeastern Spain

J. Jódar [a,*], F.M. Rubio [a], E. Custodio [b], S. Martos-Rosillo [a], J. Pey [c], C. Herrera [d], V. Turu [e], C. Pérez-Bielsa [a], P. Ibarra [a,†], L.J. Lambán [a]

[a] Geological and Mining Institute of Spain (IGME), Spain
[b] Groundwater Hydrology Group, Department of Civil and Environmental Engineering, Technical University of Catalonia (UPC) & Royal Academy of Sciences of Spain, Spain
[c] ARAID, Instituto Pirenaico de Ecología (IPE-CSIC), Spain
[d] Universidad Bernardo O'Higgins, Centro de Investigación y Desarrollo de Ecosistemas Hídricos, Santiago, Chile
[e] Marcel Chevalier Earth Science Foundation, Andorra

HIGHLIGHTS

- Regional groundwater flow lines discharge into the Salada de Chiprana Lake.
- Groundwater discharging into the lake is recharged at the Iberian Range slopes.
- Groundwater represents 13% of the total inflows into the Salada de Chiprana Lake.
- The lake behaves as a flow-through system rather than a closed endorheic basin.
- Lake water salinity controlled by evaporation, return flows and groundwater discharge.

GRAPHICAL ABSTRACT

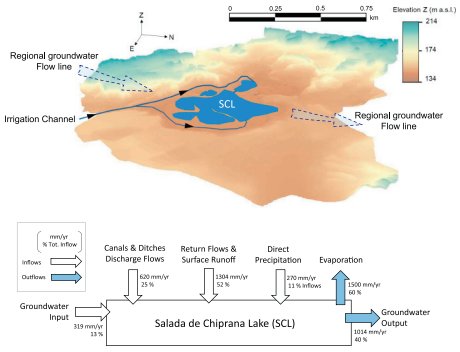

ARTICLE INFO

Article history:
Received 5 February 2020
Received in revised form 18 April 2020
Accepted 18 April 2020
Available online 22 April 2020

Editor: Damia Barcelo

Keywords:
Arid lands
Saline lake
Algal mat
Groundwater role
Flow-through lake
Stable isotopes

ABSTRACT

Most of the athalassic saline and hypersaline lakes are located in arid and semiarid regions where water availability drives the hydrological dynamics of the lake itself and the associated ecosystems. This is the case of the Salada de Chiprana Lake, in the Ebro River basin (Spain). It is the only athalassic permanent hypersaline lake in Western Europe, and where rare and endangered bacterial mats exist. This work presents a robust hydrogeological conceptual model for the lake system. The model evaluates the contribution of groundwater discharge to the whole water budget and explains the hydrological behaviour of the lake system. The lake behaves as a flow-through system rather than a closed basin. About 40% of total water outflow from the lake occurs as groundwater, whereas evaporation accounts for the remaining 60%. The surface water inflows are variable, but the groundwater contribution seems almost constant, amounting to 13% of the average total water inflow and contributing 1.9% of salt income. The high water salinity of the lake is controlled by evaporation, by saline water inflows from irrigation return flows, and the by groundwater outflows. The role of groundwater should be taken into account when drafting the water and land planning, once the conditions for the conservation of the algal mats are defined. A major contribution of this study is the water balance in the Salada de Chiprana Lake, which is consistent with a

* Corresponding author at: C/Manuel Lasala, 44. 9°B, 50006 Zaragoza, Spain.
E-mail address: j.jodar@igme.es (J. Jódar).
† Deceased.

https://doi.org/10.1016/j.scitotenv.2020.138848

robust hydrogeological conceptual model defined upon scarce hydrogeological, hydrochemical and isotopic data in the local context as conditioned by the regional behaviour. The water balance is a key tool to help to correctly manage this unique athalassic saline lake, and the approach used here can be extrapolated to other similar ecosystems around the world.

1. Introduction

Athalassic (non-sea originated) hypersaline environments constitute a feature of the landscape of arid and semiarid regions all over the world (De Wit, 2016). They include streams, wetlands and lakes without a direct connection to the sea and present a hydro-chemical composition that differs greatly from that of diluted or concentrated seawater. Most of these hypersaline lakes of continental origin are ephemeral as they are mainly found in endorheic areas that are very sensitive to climate variations, tectonics, volcanism, sedimentation and erosion. Besides, these lakes evolve seasonally between shallow water bodies in wet periods and dry salt flats during dry periods. These seasonal water level fluctuations generate seasonal variations in lake water temperature and salinity (Berlanga Herranz et al., 2017; Herbst, 2001; Jellison et al., 2008) that in turn affect the biological dynamics of the lake-depending ecosystems.

Completely self-sustaining ecosystems of photosynthetic microbial mats may inhabit such environments. When they are pristine, they represent ancient relicts of the first biological communities in which oxygenated photosynthesis might have appeared (Des Marais, 2003). These microbial mats are excellent natural laboratories that help to understand the primal conditions from which these mats have evolved and even to reveal the biological activity or "biosignatures" in exoplanet explorations through the fingerprint of the gaseous emissions generated by the biological activity (Meadows et al., 2018).

The Salada de Chiprana Lake (SCL) is an endorheic basin located at the right side of a sloping plain apron in the central Ebro River basin (NE Spain). The endorheic watershed has been subjected to changes of soil uses over the last 150 years, mainly driven by rain fed and irrigated agricultural activities to produce fodder. The SCL has been used to discharge excess water from the canals and drainage from the irrigated areas, a critical water surplus in this arid zone that helps the SCL to be the only permanent athalassic shallow hypersaline lake known in Western Europe. Moreover, the lake hosts benthic cyanobacterial mat communities of Coleofasciculus chthonoplastes, which can be considered as a living stromatolite (De Wit, 2016). These mats have been on the research focus over the last two decades (Guerrero et al., 1991; Vidondo et al., 1993; Jonkers et al., 2003; De Wit et al., 2005; Polerecky et al., 2007; Ragon et al., 2014; Iniesto et al., 2017). Other important biological features of the SCL include the rare benthic macrophyte Lamprothamnium papulosum, whose debris allow the bacterial mats to get developed, and the green phototrophic sulphate-reducing bacterium (Chlorobium vibrioforme) that can be found developing their activity in the deepest anoxic zones of the SCL. Besides, in the SCL exist a large population of brine shrimps (Artemia parthenogenetica) that control the fast growing of phytoplankton, thus maintaining water transparency, which along with not large water salinity variations, are required conditions for the benthic macrophytes to live.

In the 1990s, after realizing the relevance of the bacterial mats, the scientific community called for regulation of water inflows into the lake to preserve the SCL mat ecosystem (Guerrero et al., 1991; Guerrero and De Wit, 1992; Vidondo et al., 1993; Jonkers et al., 2003). A management plan started in 1993 with the objective of re-establishing the close-to-natural climatic and hydrological conditions by preventing direct inflows of surplus irrigation water into the lake. Nevertheless, as the management plan advanced, a decreasing trend in the lake surface area along with an increasing trend in the lake water salinity was reported, thus jeopardizing the integrity of the whole biological ecosystem. To reverse these trends, additional inflows of fresh water into the SCL have been envisioned, based in some hydrological characterization studies (DGA, 1994, 2012, 2017). However, those studies considered only surface water sources and processes (e.g. evaporation), while neglecting the contribution of groundwater to the lake water and dissolved salts balance. Nevertheless, it is known that the small endorheic salt lakes and playas, locally known as "saladas", located in both banks of the Ebro River plain, correspond to highly-mineralized diffuse groundwater discharges, which may be locally important (Ibáñez, 1975a, 1975b; Davis, 1994; Sánchez et al., 1999; Samper et al., 1993; Castañeda and García-Vera, 2008). To correctly manage the water storage and salinity of the SCL, a robust Hydrogeological Conceptual Model (HCM) is needed. The HCM is the basis of the hydrogeological system analysis and considers in a comprehended way all the flow terms driving the hydrogeological system response (Betancur et al., 2012). Therefore, the HCM allows carrying out well-founded water and salt balances and avoids non-remediable management errors.

The objective of this work is twofold, on one hand, to stablish a robust HCM and the corresponding water mass balance (WMB) for the SCL and on the other hand, to analyse the origin of groundwater discharging in the SCL area. The applied multidisciplinary approach that integrates the analysis of hydrodynamic, geophysical, hydrochemical, and isotopic data, can be used to characterize other athalassic endorheic saline lakes in low permeability complex formations in the Tertiary. Besides, the extrapolation and modification of the HGM here developed could help to understand the origin of groundwater recharge and solute transport in areas where both groundwater functioning and mass transport are still poorly know.

This paper is organized as follows. Section 2 provides a brief geographical, climatic, geological and hydrogeological description of the study area. Section 3 presents the measured data, the analytical methods, and the different geophysical techniques applied. Section 4 shows the obtained results. Section 5 discusses the results, focussing on (A) the origin of recharge of the groundwater discharging in the lake area, and (B) the building the HCM-WMB, and (C) the implications for the lake ecosystem conservation. Section 6 presents the conclusions.

2. The Chiprana Lake area

2.1. General background

The "Salada de Chiprana" lagoon system is located in the Ebro River valley (Spain), which is bounded to the south and the southeast by the Iberian Range (Fig. 1A). Altitudes vary from 1818 m at the rangeland, down to about 115 m in the Ebro River. The long sloping plain is an apron between about 800 m and the Ebro River, although in detail it is a carved surface due to erosion.

The lagoon area is composed by a set of ephemeral wetlands and small lakes, which are hydrologically connected to a main lake, the Salada de Chiprana, which gives its name to the system. The lake has a surface area from 17 to 36 ha, is 4.2 to 5.6 m deep and has a tributary basin of 768 ha. The SCL system is a protected area. Since 1994 it is a Ramsar Convention wetland site, since 1997 it is a site of community interest (SCI) according to the Habitat Directive of the European Union, and since 2006 it is a Natural Reserve of the Aragón Regional Government.

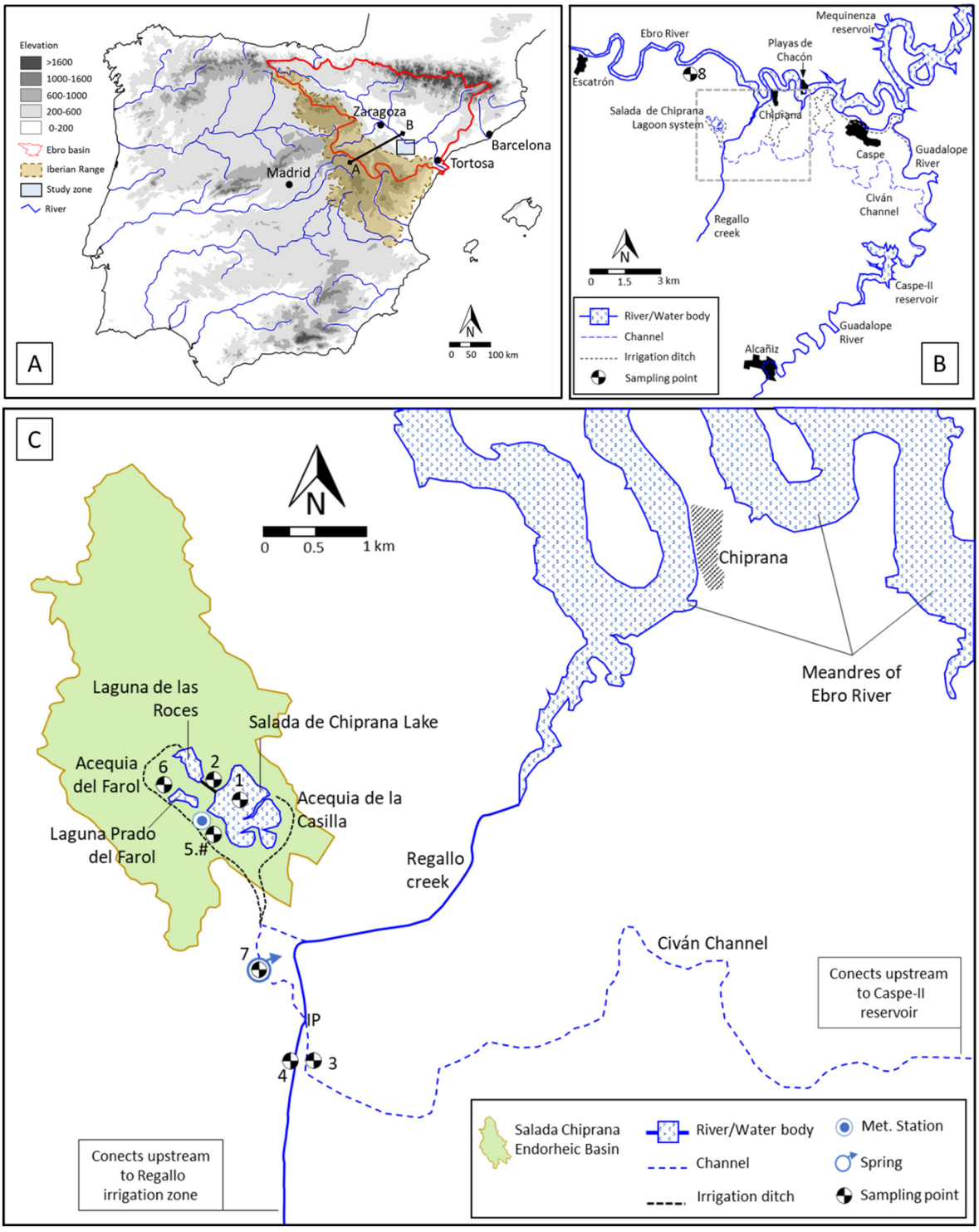

Fig. 1. Study area setting. (A) Major geographical features of the Iberian Peninsula, including the main rivers and mountain ranges. (B) Location map of the Salada de Chiprana lagoon system and its surroundings. (C) Map of the Salada de Chiprana endorheic basin and the associated lagoon system including the SCL. See Table 1 for the identification of the sampling points. Sampling point 5 is a set of 4 close by boreholes fitted as piezometers.

The irrigated areas are ubiquitous in the surroundings of the SCL. Their altitude varies between 143 and 157 m, while the lake is at 138 m and the closest Ebro River stretch is at 115 m. Irrigation water comes from outside and has been channelled to the endorheic watershed through the Acequia de Farol and the Acequia de la Casilla irrigation ditches. At the intersection point (IP in Fig. 1C), manually operated sluices allow feeding both canals either through the Civán Channel or from the water available at the Regallo irrigation zone. The Laguna de las Roces is a small oligohaline lake, which connects to the SCL through the small Roces Canal.

According to the Köppen–Geiger classification (Peel et al., 2007), the climate is arid and hot (AEMET/IM, 2011), which is characterized by very hot summers and quite cold dry winters. For the period 1990–2012, the mean monthly temperature measured at the

meteorological station of the SCL (Fig. 1C) ranged between 4.8 and 25.8 °C, the mean annual precipitation was 264 mm/yr and the average pan evaporation was 1500 mm/yr (Fig. 2; DGA, 2012).

2.2. General geological and hydrogeological background

The Iberian Range is an intraplate mountain chain made up of materials belonging to the period comprised between the Paleozoic and the Cenozoic. Jurassic and Cretaceous carbonated rocks predominate in this area (Sánchez et al., 1999). This mountain range conforms the natural southern margin of the Ebro River basin, which is a foreland basin generated during the Palaeogene (Muñoz-Jiménez and Casas-Sainz, 1997). In the southern margin of the basin, the Neogene deposits, which may be up to ~1000 m thick, overlay the existing Palaeogene units and cover unconformably the Paleozoic and Mesozoic materials of the Iberian Range (Fig. 3). This allows defining the regional hydrogeological model. It consists of a mountain block with permeable carbonate formations receiving significant recharge, and a long plain apron to the north, bounded by the Ebro River. Groundwater discharge from the mountain block is mainly produced at its periphery through small rivers and springs. Little groundwater is transferred to the low permeability plain apron, but some flow can be expected to discharge directly to the Ebro River or feed small springs and shallow water table areas. The deepest formations behave as confined, but may recharge the formations above by upward seepage and through fractures. No good deep aquifers are expected in the area. The groundwater renovation times are presumably of hundreds to thousands of years. Little local recharge is expected in the plain apron due to the arid environment (Fig. 2) and retentive soils.

Regional aquifer studies are scarce and uncertain. Groundwater balance results derive mainly from large-scale rainfall-runoff models, as those done in the Ebro River basin for water planning or from Iberian peninsula-scale atmospheric chloride deposition balances, as presented by Alcalá and Custodio (2015) and RAEMIA (2019). These calculations take into account the export of Cl with surface runoff. Precipitation varies between 450 and 550 mm/yr in the Iberian Range, down to 250–350 mm/yr in the Ebro River depression. According to local circumstances, the calculated recharge decreases from up to 250–300 mm/yr in the Iberian Range to <100 mm/a in the Ebro River plain, which may be as low as 10 mm/yr or less in the driest areas with clayish soils. After Alcalá and Custodio (2008, 2014, 2015), the average regional rainfall contains 0.4 to 4 mg/L Cl and contributes a total wet and dry deposition of about 0.5–1.5 g m^{-2} yr^{-1} Cl. The coefficient of variation of recharge is estimated between 0.25 and 0.3.

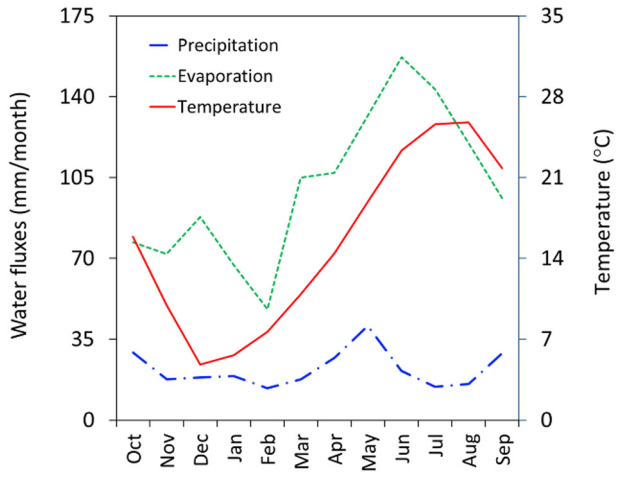

Fig. 2. Seasonal variation of average precipitation, evaporation from class-A tank, and monthly average temperature measured at the meteorological station of the SCL.

2.3. Local hydrological and hydro-geological settings

The Salada de Chiprana lagoon system is located on the Tertiary, detritic Caspe Formation (Quirantes, 1971, 1978). Here, the predominant materials are alternating marls and lutites, including calcite ($CaCO_3$), dolomite ($CaMg(CO_3)_2$), sandstones and some layers of micro-conglomerates, gypsum ($CaSO_4 \cdot 2H_2O$)/anhydrite ($CaSO_4$) and glauberite ($Na_2Ca(SO_4)_2$), with a complex and heterogeneous distribution (Salvany et al., 2007; Guerrero et al., 2013), as shown in Fig. 4. From a geomorphological point of view, the study area has a moderate to gentle large-scale relief. The high areas correspond to paleochannels whose dominant lithology consists on sandstones, conforming thick horizons containing some micro-conglomeratic levels. Such structures present a moderate permeability, while the depressed zones correspond to low permeability fillings in which the dominant materials are marls with intercalations of clays, sandstones and gypsum (DGA, 1994).

The Chiprana agricultural area is irrigated with water imported through the Civán Channel, a diversion of the Guadalope River, which in turns is fed by the Caspe-II surface water reservoir (Fig. 2B). The irrigation return flows generated in the area are diverted to the SCL. These inflows, along with the direct precipitation and the regional groundwater discharge into the lake make the SCL permanent. Otherwise, the arid conditions prevailing in the zone would force the SCL to follow a seasonal flooding trend. The average water level in the SCL for the period 2004–2011 is 138.5 m above sea level (a.s.l.). This level varies seasonally <1 m and up to 1 m in the whole data period, without any clear trend. It is not possible to know if the water level in the SCL exceeded any time in the past the limits of the current endorheic basin because the deflation and abrasion generated by the prevalent strong local wind known as "Cierzo", along with the intense agricultural activities conducted in the area since the 17th century, have eroded the possible typical stepped sequences associated to different lacustrine levels at the margins of the SCL. Nowadays, the SCL is an endorheic hydrological system that has no other visible water outflow than evaporation from the lake.

The lagoon system is close to the Ebro River, whose right bank receives regional groundwater discharge from the Iberian Range (Sánchez et al., 1999), in agreement with the vertical head profile defined by the four short-screened piezometers located at the southern boundary of the SCL (Fig. 5). There is a 0.27 upward vertical head gradient.

The piezometric data do not show temporal trends. The deeper piezometer head is 13 m above lake level. There are small seasonal effects that seem to dampen with screen depths. However, piezometer S-2, screened around the lake level, shows some discrepancies with respect to the lake level and a recent draw drown trend that brings the local water table about 3 m below the nearby lake level. A possible explanation is that the lake level is a composite value and S2 is only representative of the local water table close to the lake, in that case near the outflow stretch.

The SCL water salinity derives mainly from three sources: (1) agricultural activities, mostly evapo-concentration of return irrigation water, (2) surface water inflow incorporating soil salts lixiviated by rainwater, and (3) groundwater salinity. The hydrochemical facies of water in the SCL is similar to that of most of the saline flats in the central Ebro basin. It is commonly hypersaline (Fig. 6), of the magnesium-sodium sulphate-chloride type, with seasonal variations mainly driven by evaporation and freshwater inputs to the lake (Vidondo et al., 1993). The dominance of Mg in lake water agrees with what is observed in the algal mats. There is dispersed data from 1987 to 2004, which show 40 to 90 g/L of total dissolved solids (TDS). There is not a clear evolution trend. However, data of 2016, obtained during the present study, showed less saline water, between 10 and 40 TDS. Before performing the geophysical surveys, it was measured an electrical conductivity of 70 mS/cm (about 40 g/L TDS).

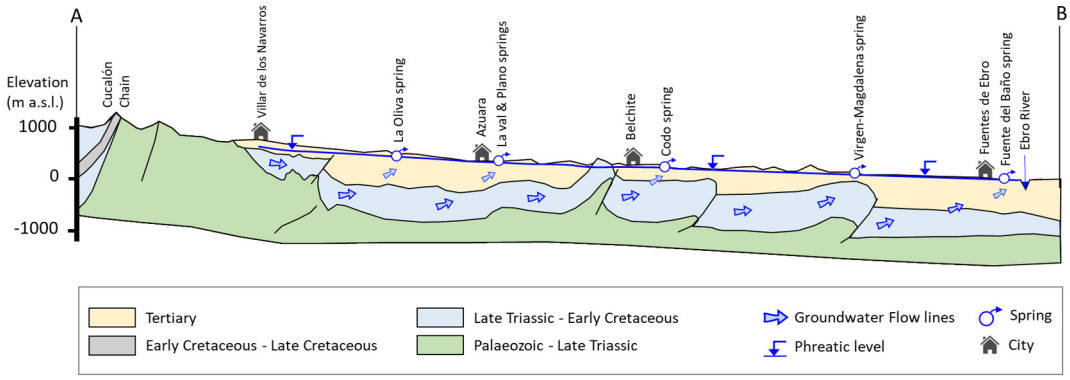

Fig. 3. A-B hydrogeological section (Fig. 1A) of the contact between the Iberian Range and the Tertiary Ebro Basin (modified from Sánchez et al., 1999). The Jurassic and Cretaceous carbonates constitute the main regional aquifer.

3. Methods and materials

3.1. A water sampling surveys

Aside from meteorological data and preliminary evaluations for water planning by the Ebro Basin Water Authority, relevant regional hydrogeological information for the present study area is very scarce. The isotopic composition of rainwater is determined monthly since 2000 by the IAEA-GNIP worldwide network, although last available data is for 2011. Since 2015, monthly rainwater sampling for chemical and isotopic analysis are collected in a rain gauge (pluviometer) operated by the Geological and Mining Institute of Spain in Escatrón (P8 in

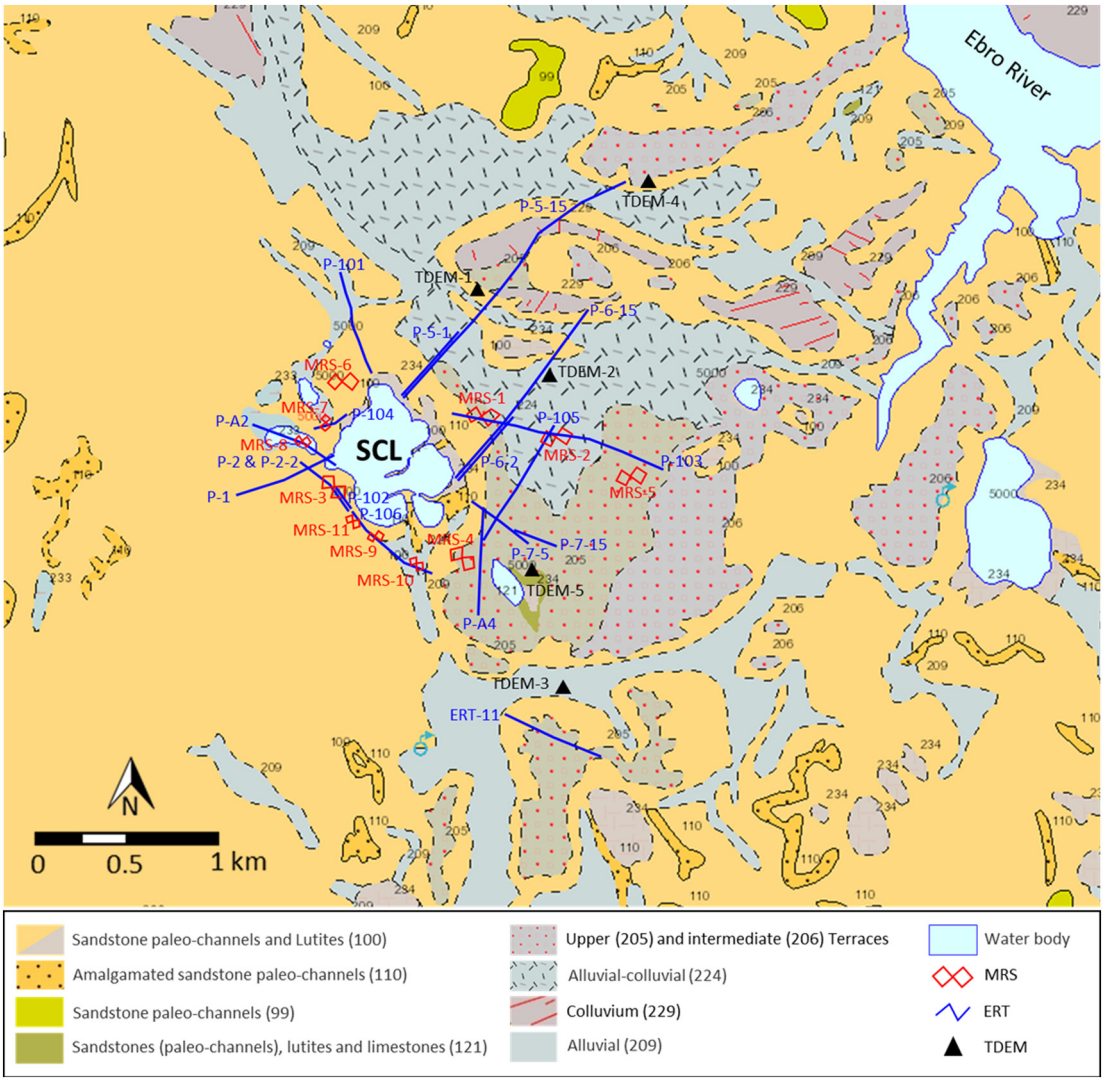

Fig. 4. Geological map of the SCL area (GEODE, 2011) and location of geophysical measurements. Red loops: proton Magnetic Resonance Sounding (MRS); blue lines: Electrical Resistivity Tomography (ERT) profiles; and black triangles: Time Domain Electromagnetic Soundings (TDEM). (For interpretation of the references to colour in this figure legend, the reader is referred to the web version of this article.)

Fig. 1B). Water level in the SCL and in the piezometers nearby are measured monthly by the "Reserva Natural Dirigida de las Saladas de Chiprana" [Directed Managed Natural Reserve of the Saladas de Chiprana] (DNRSC) since 2009. The piezometers (S1 to S4) are installed in close by boreholes located 5 m southwards from the SCL (Fig. 1C, point "5.#"). The shallowest piezometer is a common one but the other three are grouted tubes down to the screen and capped to avoid overflowing. The heads are measured by means of pressure gauges.

To complement the information needed for the objectives of this study, 5 campaigns of chemical and isotopic sampling of precipitation, surface water and groundwater were carried out near the DNRSC between April and December 2016. A total of 68 water samples have been analysed (Table 1). The water sampling points considered in this study to explore the main geochemical and isotopic signatures of all water sources contributing to the SCL water balance are shown in Fig. 1, while Table 1 shows their characteristics. Prior to groundwater sampling, the piezometers were purged by pumping at least three times the borehole volume and until temperature (T) and electrical conductivity (EC) were stable.

The chemical analyses were carried out in the Laboratory of the Geological and Mining Institute of Spain (IGME), in Madrid. None of the water samples were filtered or acidified in the field. In all cases, the electrical conductivity (EC), pH and temperature (T) were measured on site. All water samples were stored in polyethylene bottles, transported to the laboratory on ice and maintained at 4 °C until analysis.

In the laboratory, the pH and EC (electrical conductivity) measurements were made by electrometry (pH meter HM model 781 and CRISON model MICRO CM2201, respectively); the bicarbonate, calcium and magnesium concentrations were determined by molecular absorption in continuous flow using an ALLIANCE autoanalyser, model INTEGRAL PLUS; the chloride, sulphate and nitrate concentrations were determined by ionic chromatography; the sodium and potassium concentrations were determined by atomic absorption spectroscopy with a VARIAN equipment model SPECTRA AA 220; and the carbonate ions were determined by titration. The measured chemical components were Na^+, K^+, Ca^{2+}, Mg^{2+}, Cl^-, HCO_3^-, NO_3^- and SO_4^{2-}. In all cases the laboratory measurement error was 0.01 mg/L.

The water stable isotope analyses were carried out in the Laboratory of the Interdepartmental Investigation Service (SIdI) of the Autonomous University of Madrid (Madrid), with a SMS (small mass spectrometer), a Delta Plus Advantage model by Finnigan MAT. $\delta^{18}O$ was determined through the water–CO_2 equilibration technique and δ^2H through the water–H_2 equilibration technique using a platinum catalyst. The analytical uncertainties for $\delta^{18}O$ and δ^2H are $\pm 0.2‰$ and $\pm$ 1.0‰, respectively. The laboratory standards were regularly calibrated and referred to the VSMOW standard (Vienna Standard Mean Ocean Water).

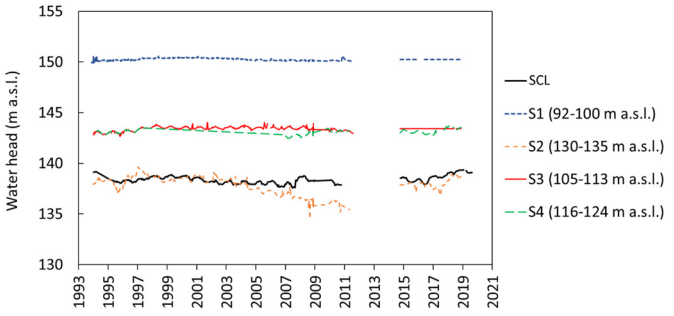

Fig. 5. Evolution of the SCL water level and piezometric levels measured in the piezometers S1 to S4 for the period 1994–2011 (data provided by the Servicio Provincial de Agricultura, Ganadería y Medio Ambiente in Zaragoza, Gobierno de Aragón). The legend indicates the elevation of the screened interval of the piezometers. See the situation in Fig. 1C.

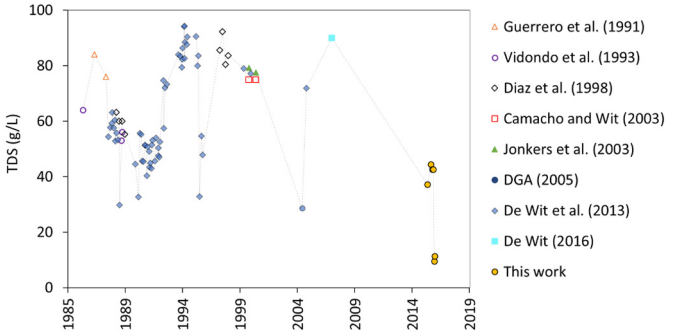

Fig. 6. Variation of the total dissolved salt concentration (TDS) in the SCL, as reported by different authors.

Geochemical calculations have been conducted with the PHREEQC program (Parkhurst and Appelo, 2013).

3.2. Geophysical characterization of the aquifers

3.2.1. Electrical resistivity tomography

The Electrical Resistivity Tomography (ERT) method provides a 2D model of the ground by defining the geometry of an aquifer in areas of moderate geological complexity. It is a widely applied geophysical exploration method to investigate wetlands and endorheic hydrological systems (Plata, 1999; Rubin and Hubbard, 2006; Andrews et al., 1995; Owen et al., 2006; Rein et al., 2004; Descloitres et al., 2008; Ruiz et al., 2006; Rubio Sánchez-Aguililla et al., 2017).

In the framework of this study, 19 ERT profiles were performed in two field surveys conducted in July 2016 and September 2017 (Fig. 4, Table 2). Some of the ERT profiles were oriented following a SW-NE direction, according with the assumed regional groundwater flow lines (Sánchez et al., 1999). The apparent resistivity data were collected with an ABEM AS4000 instrument, using the multi-electrode Lund system. To obtain the best estimate of the 2D true resistivity distribution beneath each profile, the data obtained has been processed and inverted, taking into account the soil surface topography through the program Res2DInv version 3.71 (Loke, 2001), and edited with the program Erigraph, version 2.20.

3.2.2. Magnetic resonance sounding

The proton Magnetic Resonance Sounding (MRS) allows estimating soil porosity, permeability and thickness along the first hundred meters below ground surface. Besides, it is the only geophysical method that is able to directly detect the presence of free water in the ground (Lubczynski and Roy, 2003, 2007; Legchenko and Valla, 2002; Legchenko et al., 2002; Bernard, 2007; Plata and Rubio, 2007; Vouillamoz et al., 2007). The free water content is close to the water content that can be displaced under moderate hydraulic gradient, with respect to the total rock volume (Lubczynski and Roy, 2003).

A MRS survey was carried out in September 2016 for mapping groundwater in the Tertiary basement domain where the SCL is located. 11 MRS measurements were performed using a NUMIS LITE equipment (IRIS Instruments (Fig. 4). An eight-shaped loop as antenna configuration was used in all of them. The interpretation of the measured data though inversion (Yaramanci and Hertrich, 2007) was conducted with the software SAMOVAR v6.2 from IRIS. The maximum exploration depth is equal to the dimensions of the antenna, which is the length side of the larger squares in the case of an eight-shaped loop antenna configuration. For MRS-1 to MRS-1, the antenna length side was 60 m whereas for the rest of soundings it was 30 m.

Table 1
Water sampling points in the study zone.

Code	Sampling Point	Latitude (°)	Longitude (°)	Elevation (m a.s.l.)	Well depth (m)/screened interval (m)	Num. Water Samples	Water type
1	SCL	41.241516	0.181326	138	–	5	SW
2	Roces Canal	41.241814	0.186850	142	–	5	SW
3	Civán Channel	41.213783	0.179405	159	–	6	SW
4	Regallo Creek	41.213843	0.179247	159	–	6	SW
5.1	Piezometer S1	41,240,704	0.184941	142	50/42–50	4	GW
5.2	Piezometer S2	41.240704	0.184941	142	10/2–10	5	GW
5.3	Piezometer S3	41.240704	0.184941	142	38/30–38	5	GW
5.4	Piezometer S4	41.240704	0.184941	142	26/18–26	5	GW
6	Farol Well	41.241432	0.192594	144	6/0–6	5	GW
7	Fonté ooze	41.227162	0.174797	143	0	4	GW
8	Pluvio. Escatrón	41,279,720	−0.218890	160	–	18	P

SW = Surface water; GW = Groundwater; SW-G = surface water derived from upstream spring area; P Precipitation.

3.2.3. Time domain electromagnetic soundings

Time Domain Electromagnetic sounding Method (TDEM) (Kafri and Goldman, 2005) gives 1D information about the vertical resistivity distribution with a larger penetration depth than the ERT method, thus helping to determine the depth and thickness of the resistive layers.

Five TDEM soundings were conducted in September 2016 to define in depth the position of the substrate corresponding to the Tertiary materials that fill the basin where the lagoon system is located. The TDEMs were located close to ERT profiles (Fig. 4) and the position of the TDEM-3 is close to the SCL borehole, which has a geological log. The equipment used for conducting the TDEM soundings is a Phoenix Geophysics System 2000. For the 5 soundings, a single antenna loop configuration was applied. In all cases, the antenna loop size was 150 m × 150 m, except for SEDT 3, whose size was 100 m × 100 m. Measured data were post-processed with the IX1D software (Interpex, 2006), yielding a resistivity-depth curve that helps to define the soil profile structure, while allowing greater depths than those obtained with the ERT soundings.

4. Results

4.1. Results from geophysical surveys

4.1.1. Electrical resistivity tomography

The interpretation of all the electrical resistivity tomography (ERT) profiles shows very conductive sections (2–6 Ω·m) lagoon areas that were dry at the time of measurements, normally with a thickness of about 10 m. They are interpreted as sections with salt water. There is a relatively conductive (30–60 Ω·m), 20 m thick surface layer, corresponding to dry or partially saturated materials (Fig. 7A). The horizontal continuity of this layer is sometimes broken by high resistivity zones (>260 Ω·m) around the lake at the upper part of the profiles, coinciding with the presence of sandstone paleochannels. Below these structures there is a sub-horizontal low resistivity level (<30 Ω·m), up to 30 m thick, which includes small areas of even lower resistivity (4–16 Ω·m), representing water saturated levels through which groundwater may flow. Additionally, there is a medium to high resistivity zone

Table 2
Technical settings of the ERT profiles. See location in Fig. 4.

Profile	Array configuration	Electrode spacing	Profile length	Orientation	Direction[a]
P-1	Wenner	15	600	SW-NE	Parallel
P-11	Wenner ls	15	600	NW-SE	Perpendicular
P-11–2	Wenner	15	600	NW-SE	Perpendicular
P-2	Wenner	5	400	NW-SE	Perpendicular
P-2-2	Dip-Dip	5	400	NW-SE	Perpendicular
P-A2	Wenner ls	5	500	NW-SE	Perpendicular
P-A4	Wenner	15	600	N-S	Subparallel
P-5-15	Wenner ls	15	1800	SW-NE	Parallel
P-5-1	Wenner	5	400	SW-NE	Parallel
P-6-15	Wenner ls	15	1200	SW-NE	Parallel
P-6-2	Wenner ls	5	400	SW-NE	Parallel
P-7-15	Wenner	15	600	NW-SE	Perpendicular
P-7-5	Wenner	5	400	NW-SE	Perpendicular
P-101	Wenner	5	600	NNW-SSE	Subparallel
P-102	Wenner-Schlumberger	2.5	200	NW-SE	Perpendicular
P-103	Wenner	5	1250	NW-SE	Perpendicular
P-104	Wenner	2.5	200	NW-SE	Perpendicular
P-105	Wenner	5	800	SW-NE	Parallel
P-106	Wenner	2.5	650	NW-SE	Perpendicular

[a] Direction of the ERT respect to the assumed regional groundwater flow line.

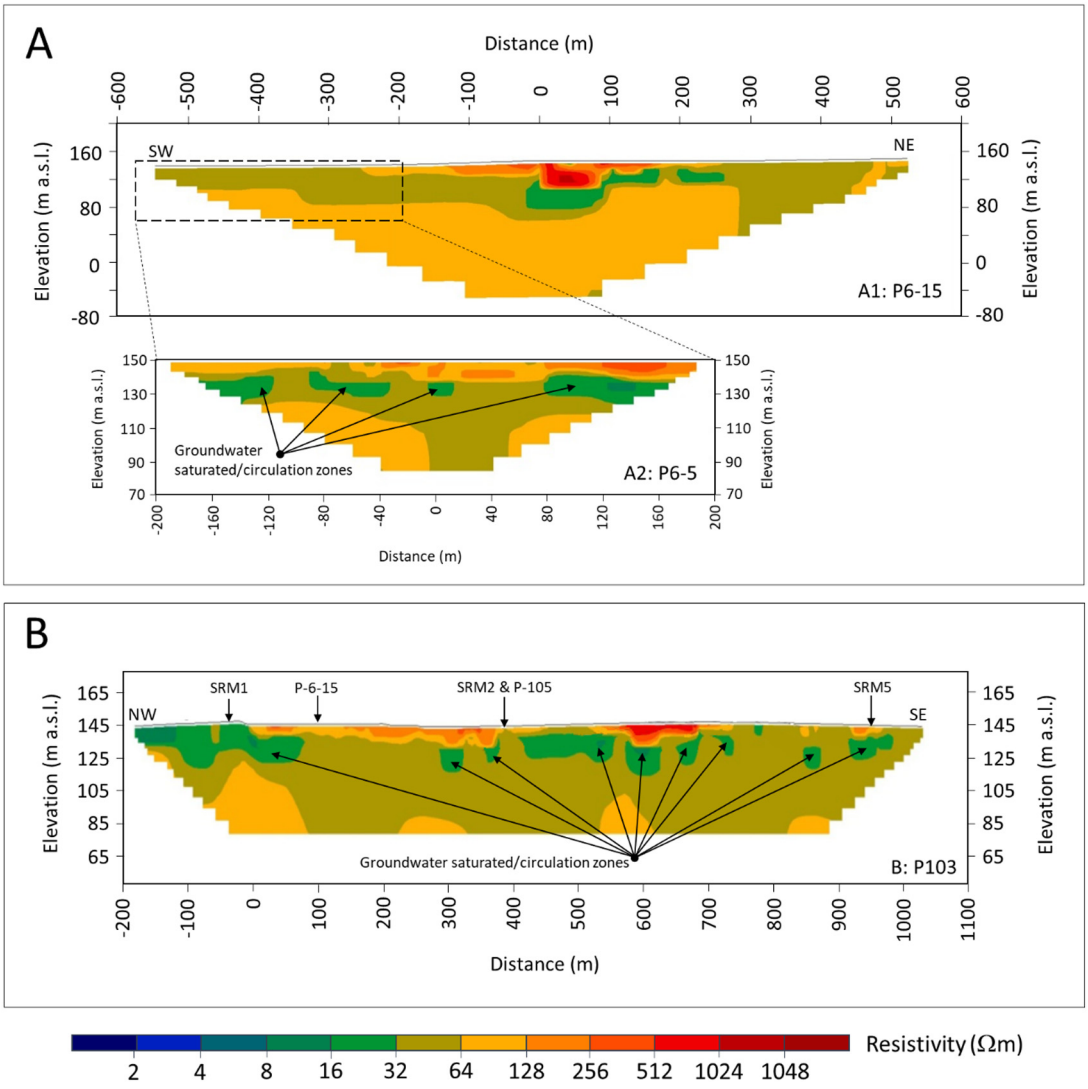

Fig. 7. Resistivity sections obtained for (A) P-6-15 and P-6-5 and (B) P-103 ERT profiles. See the location in Fig. 1. The interpretation of the other ERT profiles can be seen in Figs. SM1 to SM9 - Suppl. Mat.

(60–130 Ω·m) at the lower part of the profiles, which are related to the lutitic and/or marly materials typical of the Tertiary in the Ebro basin. Besides, the profiles have a relatively homogeneous resistive background of >50 Ω·m in which relative resistivity minima values lower than 30 Ω·m can be found at a relatively constant depth around 15 m. They correspond to levels that probably allow groundwater flow (Fig. 7B).

4.1.2. Magnetic resonance soundings

The magnetic resonance soundings (MRS) show two different zones with both a high water content and permeability (Fig. 8). The first one comprises the first 10 m deep soil layer, coinciding with Quaternary and Tertiary unconsolidated sediments that present a moderate mean permeability of 37 mm/d and a mean water content of 6%, with a low water content and an average permeability of 1 mm/d. The second zone is thicker than the first one. It is located at elevations between 130 and 100 m a.s.l. and corresponds to sandstone paleochannels. In this zone, the mean permeability is 41 mm/d and the water content is 6%. In the MRS profile shown in Fig. 8, which comprises the soundings MRS3, MRS11, MRS9 and MRS10, the permeability and free water content become higher, and the thickness increases along the profile. This trend can be also observed in terms of resistivity in the 102-106-ERT profile (Fig SM4) that runs parallel to MRS3-MRS10. At elevations lower than 100 there is a marked transition between the above-mentioned permeable and water-rich levels and the deep levels detected by the MRSs, especially in MRS3 and MRS11, where permeability drops to values close 0.1 mm/d, representing the deep Tertiary materials of the Ebro Basin.

4.1.3. Time domain electromagnetic soundings

The time domain electromagnetic soundings (TDEMs) allow the exploration of the materials in the Ebro basin at deeper lengths. All the TDEMs show an upper resistive, 15 to 40 m thick layer (Fig. 9). Below this layer there is a conductive one (15–30 Ω·m) down to 150–180 m, which is observed in all the TDEMs, except in TDEM-1 because this sounding is less penetrating. The conductivity of this layer is consistent with that of the Tertiary lutitic materials (Mazáč et al., 1985). They may behave as an aquitard. TDEM-5, which is located next to ERT-7, shows a different response. There is a resistive layer (50–60 Ω·m) right below the above-mentioned surface conductive layer. This feature correlates with the resistive layer observed in the tomographic profile. It seems to show a high electrical resistivity barrier in the area of the lagoon system. In the deepest zone explored by the different TDEMs, an unlikely conductive layer is noticed, which is interpreted as noise that distorts the final part of the soundings. In this regard, only TDEM-1 presents an 8 m thick deep conductive zone at 50–60 m depth.

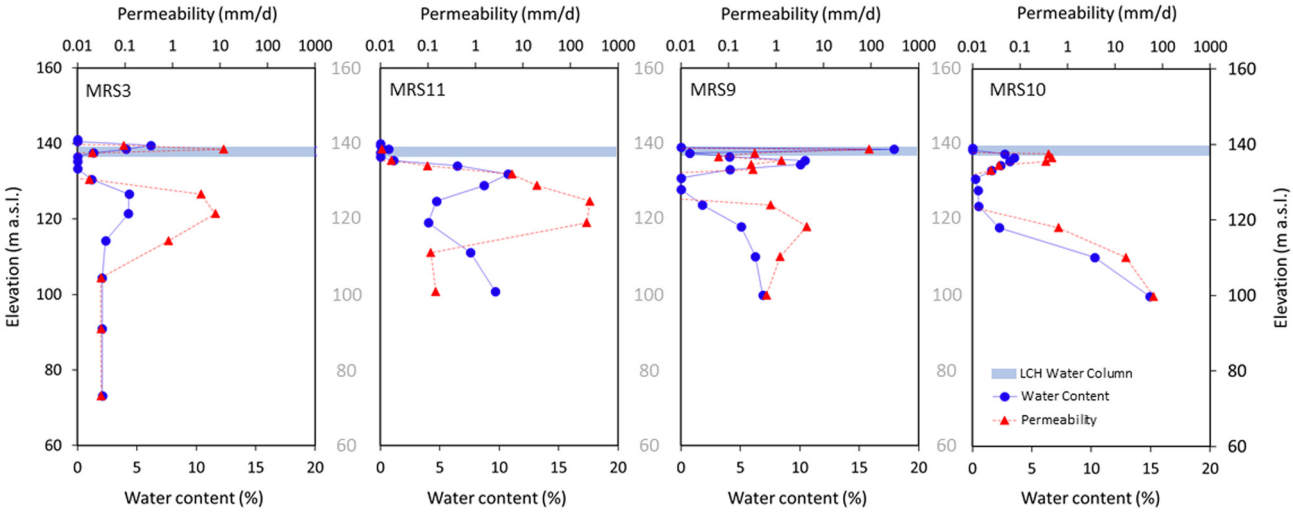

Fig. 8. Vertical profiles of water content (circles) and mean permeability (triangles) interpreted from the MRS soundings along the line in the SW boundary of the SCH defined by MRS3, MRS11, MRS9 and MRS10 along (Fig. 4). The shaded line indicates the lake water column, with the lake surface at a mean elevation of 138.5 m a.s.l. and the lake bottom at 136.7 m a.s.l. (Valero-Garcés et al., 2018).

4.2. Hydrogeochemical results

In the 5 field campaigns conducted between April and December 2016, the mean EC value in the SCL was 70 mS/cm. This value is at least one order of magnitude higher than the EC values measured in the other sampling points (Table SM1 - Suppl. Mat.). The mean EC values associated to the other sampled surface water sources (Roces Canal, Cián Channel and Regallo Creek) is relatively low. Out of the water samples from SCL, the EC associated to the other surface water sources is lower than in groundwater.

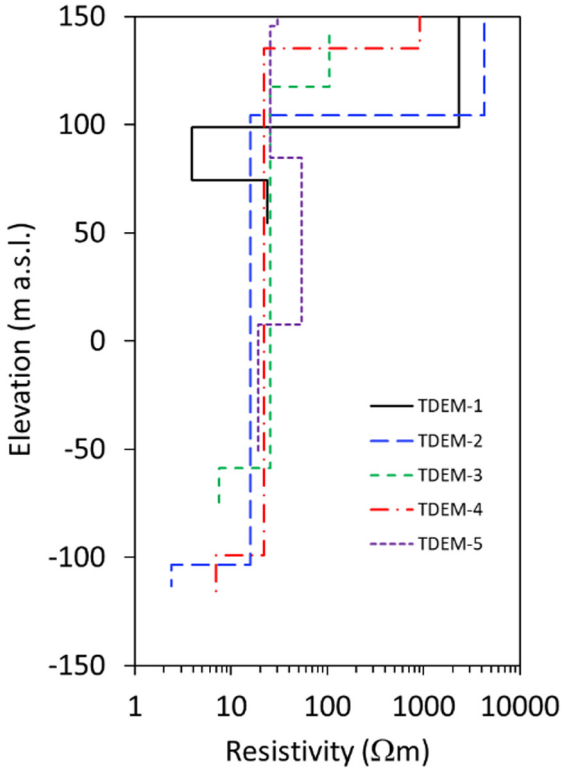

Fig. 9. Vertical soil resistivity profiles obtained from the TDEM soundings.

The average chemical composition of the analysed waters in the sampled points is shown in Fig. 10. In general, the water is of the calcium-sulphate type. The chemical concentrations are mostly steady in time (see Figs. SM10 and SM11 - Suppl. Mat.) and vary similarly within one order of magnitude for the different water sampled points. The SCL water is the exception as it is variable and of the sodium-magnesium-sulphate-chloride type. Fig. 10 includes the average composition of rainwater in Escatrón, which is assumed representative of rainfall in the area.

With the help of the program PHREEQE and using the field pH values, different saturation indices relative to several minerals have being calculated (not shown). Sampled waters are close to saturation with respect to aragonite, calcite and silica. There is a small oversaturation with respect to dolomite, which is more defined for the lake due to evaporation and the slow kinetics. There is a trend to undersaturation in the Fonté ooze. All waters are close to saturation relative to gypsum, except for the moderately oversaturated lake water, and are highly unsaturated relative to halite.

The most relevant ionic relationships that describe the hydrogeochemical behaviour associated to the SCL hydrological system are presented in Fig. 11. The concentrations are expressed in meq/L (denoted by the prefix r). The close relationship between rNa and rCl (Fig. 11A), with a slight rNa deficit, points to the deposition of the marine aerosol as the origin of both solutes in both surface water and groundwater samples. Table 3 shows the mean Cl content for the sampling points. Regardless of their origin, the analysed water samples have a smaller variability in Ca (Fig. 11B), because they are saturated. Therefore, it precipitates when there is an additional supply of Ca. On the other hand, Mg is concentrated along with Cl in SCL (Fig. 11C), with a ratio rMg/rCl ~1. In the other sampled points, Mg is somewhat less than Cl. There is a deficit Mg with respect to SO_4 (Fig. 11F). Sulphate is concentrated in the SCL along with chloride (Fig. 11D), with a ratio $rSO_4/rCl \sim 1$. In the rest of the points, rSO_4 exceeds rCl. The ratio rCa/rSO_4 for SCL (Fig. 11E) is close to 1, indicating a concentration process in the lake. Besides, Ca shows a significant deficit respect to SO_4, pointing to the calcium precipitation process in the SCL.

4.3. Water stable isotopes

The isotopic content of rainfall water samples taken in the rain gauge of Escatrón (Point 8, Fig. 1B; Table 1) in the period 2015–2017 shows a seasonal evolution (Fig. 12A), with a heavier isotopic composition in

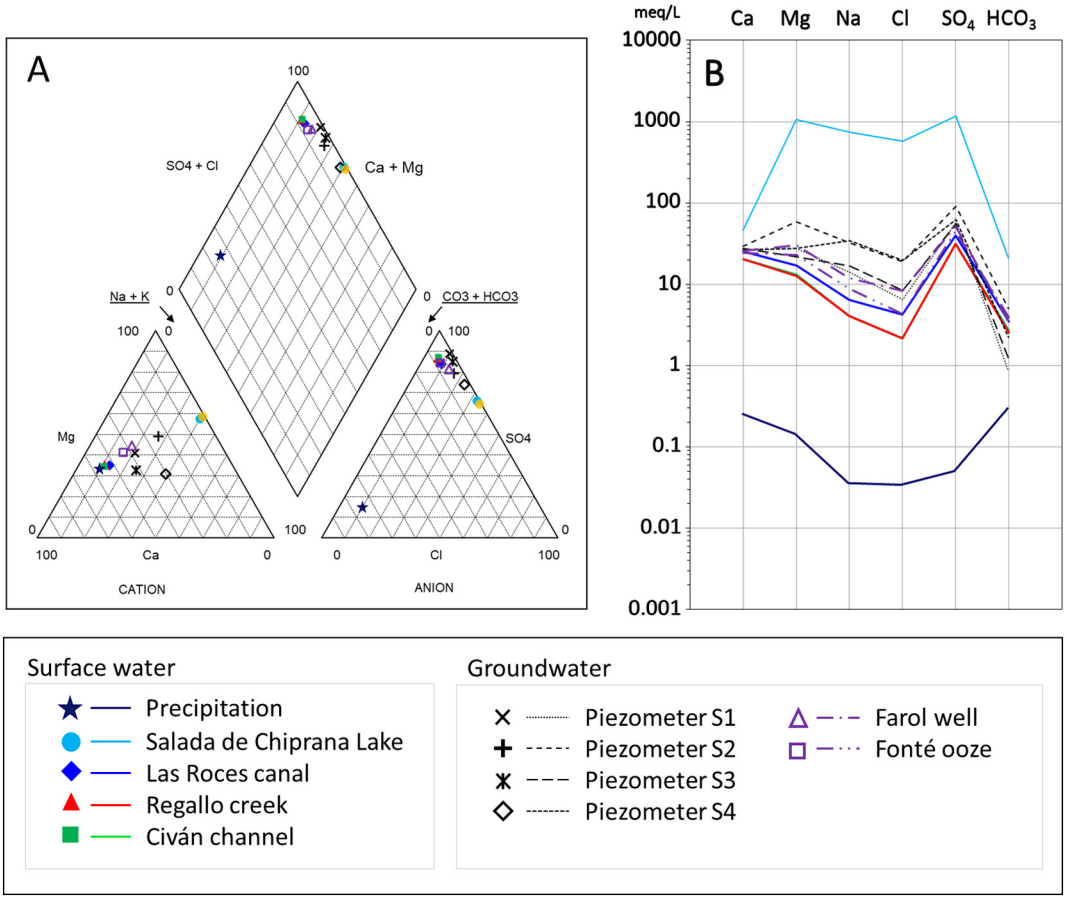

Fig. 10. Piper (A) and Schoeller-Berkaloff diagrams (B) for the average hydrochemical composition in the different water sampling points during the 2016 field campaign.

summer and lighter in winter. This time series is not long enough to estimate accurately the long-term average isotopic content in precipitation (δ_P) for the study area. For a more detailed approach, the GNIP-interpolated $\delta_P(t)$ time series is generated by using, (1) the isotopic content in precipitation measured in the rain gauge of Escatrón during the sampling survey, and (2) the interpolation of the monthly time series of isotopic content in precipitation measured in the neighbouring IAEA-GNIP meteorological stations of Zaragoza and Tortosa (Fig. 12A), not far from the study area (Fig. 1A). The GNIP-interpolated mean δ_P values for $\delta^{18}O$, $\delta^{2}H$ and deuterium excess (d) are −5.3‰, −36.0‰ and 6.1‰, respectively. The d is lower than 10‰, which is the value corresponding to the Global Meteoric Water Line (GMWL, Rozanski et al., 1993). This is a consequence of the isotopic content measured during the warm season in both the IAEA-GNIP meteorological stations and the rain gauge of Escatrón. In summer, the raindrops partially evaporate during the fall, when the air is isotopically non-equilibrated with water vapour at low relative humidity (Fig. 12B), as already observed in other parts of the Iberian Range (Moreno et al., 2014) and elsewhere (RAEMIA, 2019). This is a relevant process in semi- arid regions (Araguás-Araguás et al., 2000).

Fig. 13 shows the average values of $\delta^{18}O$ and $\delta^{2}H$ for precipitation and the different sampling points. The average isotopic content of precipitation and groundwater from the piezometers S1, S3 and S4 plot on the GMWL, except that for the shallowest borehole S2. The isotopic composition of groundwater is clearly lighter than that of local precipitation. Additionally, the average isotopic content of the surface water samples (SCL, Roces Canal, Cián Channel and Regallo Creek) and that of Fonté ooze and piezometer S2 groundwater samples plot on an Evaporation Water Line (EWL) of slope 4.65, which is coherent with a low moisture atmosphere. As shown in Fig. 13B, the sampled water becomes isotopically heavier and saltier as evaporation affects the surface water bodies of SCL and Laguna de las Roces, respectively (Fig. 1C). This relationship is also shyly shown in the other surface water sampling points (i.e. Regallo Creek and Civán Channel).

Similarly to the hydrochemical composition, only the surface water samples from the SCL have a variable isotopic content, whereas that of the other water sampling points remains stable (see Table SM4-Suppl. Mat.).

5. Discussion

5.1. Defining the groundwater recharge areas

Initially, the origin of groundwater discharging in the SCL was assumed to be local recharge, based on the chemical composition of the water samples from the SCL, the irrigation channels, and groundwater identified by the shallow piezometers (DGA, 1994, 1997, 2012; Valero-Garcés et al., 2000a). However, a wider perspective of the origin of groundwater flowing through the Tertiary materials of the Ebro basin is needed in order to not neglect a potentially significant component. This is something often forgot in wetland studies, but important for preservation and management. This is not new but new case studies are worthwhile to stress this importance and evaluate the relevance of the circumstances of each case, especially when local data is scarce and regional data is very sparse and do not derive from specific monitoring plans. Even in these poorly favourable circumstances, some quantification is possible by careful study of what is available.

The regional hydrogeological area is only 90 km apart from the Mediterranean coast, in the Ebro Delta and Tortosa, in NE Spain. Therefore, the airborne marine aerosol can reach the wetland area, although attenuated by the Catalan Costal Range barrier that runs parallel to the coast line from the Ebro River mouth northwards.

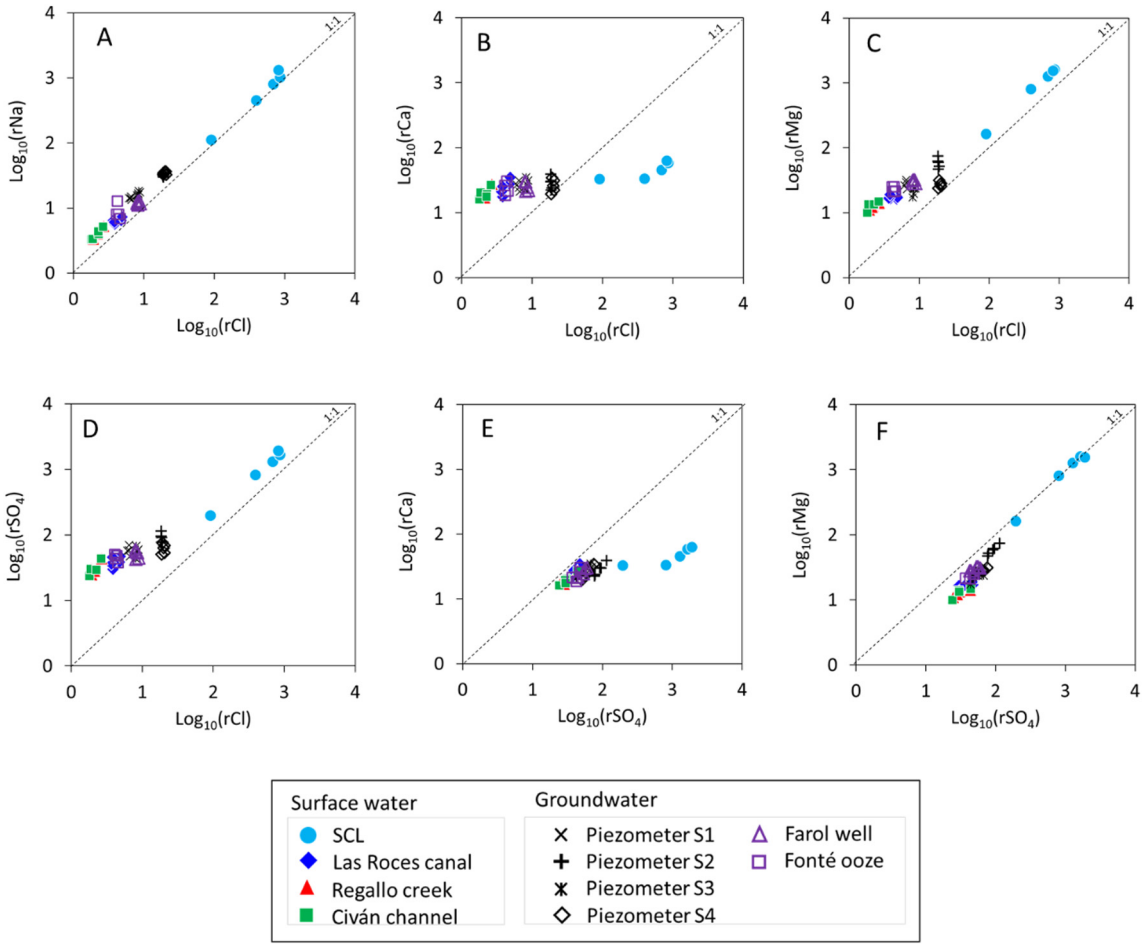

Fig. 11. Relationships between (A) log(rNa) and log(rCl), (B) log(rCa) and log(rCl), (C) log(rMg) and log(rCl), (D) log(rSO_4) and log(rCl), (E) log(rCa) and log(rSO_4), (F) log(rMg) and log (rSO_4) for the field campaigns conducted in 2006. (r = meq/L).

The study area is well known for extreme climate conditions and strong persistent winds that move local soil particles, part of which come from the gypsum and glauberite-rich formations in the Ebro depression. The consequence is a rain that partly has a marine footprint (with recirculation), but is dominated by local dust contributing Mg-rich carbonates and sulphates. This fact influences the chemical composition of recharge by evapo-concentration in the soil. Except for calcite and dolomite dissolution in the dust and the soil by soil CO_2, no other

Table 3
Average chloride content in waters around the SCL for the sampling period from April to December 2006.

Code	Sampling point	Chloride content (mg/L)	Comments
	SCL	20,477	Recent values (3–30 g/L)
1	Roces Canal	149	Civán Channel and Regallo Creek water mix
2	Civán Channel	76	From a surface reservoir
3	Regallo Creek	77	From a local discharge
4	Piezometer S2	666	Shallow borehole
5.2	Piezometer S4	704	Second shallow borehole
5.4	Piezometer S3	298	Third shallow borehole
5.3	Piezometer S1	231	Deep borehole
5.1	Farol Well	296	Large diameter shallow well
6	Fonté ooze	154	Possible deep discharge
7	Pluvio. Escatrón	1.2	Rain collector
8			

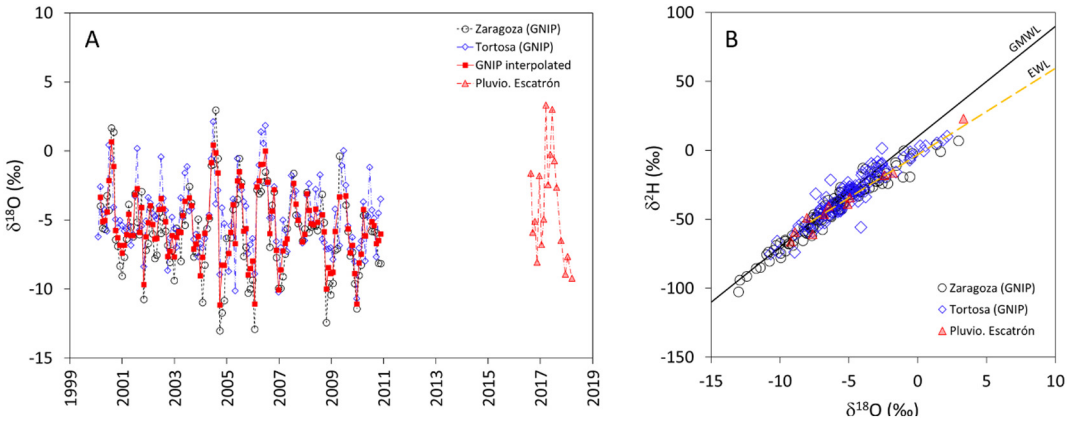

Fig. 12. (A) Time series of $\delta^{18}O$ isotopic content in precipitation measured in the IAEA-GNIP meteorological stations of Zaragoza (circles) and Tortosa (diamonds), and measured in the rain gauge of Escatrón (triangles). They are interpolated for Chiprana (solid squares) based on the measured time series of Zaragoza and Tortosa, which are maintained by the CEDEX. (B) Isotopic composition of precipitation in the IAEA-GNIP meteorological stations of Zaragoza and Tortosa, and measured in the rain gauge of Escatrón. GMWL and EWL are the global meteoric and local evaporation water lines, respectively. The GMWL has slope 8 and intercept of 10‰. The EWL corresponds to the regression of the isotopic content of precipitation in Zaragoza (IAEA-GNIP) during the warm season months (i.e. precipitation water samples from months June to October (see Fig. SM12 - Suppl. Mat.). This evaporation line has a slope of 6.2.

significant mineral contributions are probable, as Tertiary saline formations are located more to the centre of the basin and the sulphate-rich Keuper formations are not expected in the region of influence. This makes a difference with the close Ports de Besei-Tortosa aquifer system, to the East, and studied in detail (Espinosa et al., 2014).

The plots of Fig. 11 show that regional groundwater gains Ca and Mg relative to Cl, while the marine ratio rNa/rCl is maintained. The ratio rSO_4/rCl is always much greater than the marine contribution, which is due to the local contribution by airborne dust. Ca in deficit relative to SO_4 due to calcite precipitation, while Mg tend to be maintained.

Water in the shallow piezometers shows a mean Cl content between of 666 and 704 mg/L (Table 3), whereas regional discharge from the Iberian Range mountain block has probably a Cl content <80 mg/L and corresponds to high elevation springs and mountain brooks, as it happens in the part of the Iberian Range to the east (Espinosa Martínez and Custodio, 2016). A coarse Cl balance points to a recharge in the Iberian Range that is higher than 15 mm/yr. Greater values could be expected in the carbonate-dominated part discharging toward the Mediterranean Sea. Local deep groundwater has a Cl content in the range of 140–250 mg/L, indicating recharge in the Iberian Range slopes and the lateral transmission. Water in the shallow piezometers is more saline and probably reflects the presence of irrigation returns, shallow water table evaporation and airborne salt dispersion around the SCL. It is not clear the contribution of sediment salts to groundwater salinity, even if transit time is possibly very long. This contribution is more likely at lower altitudes.

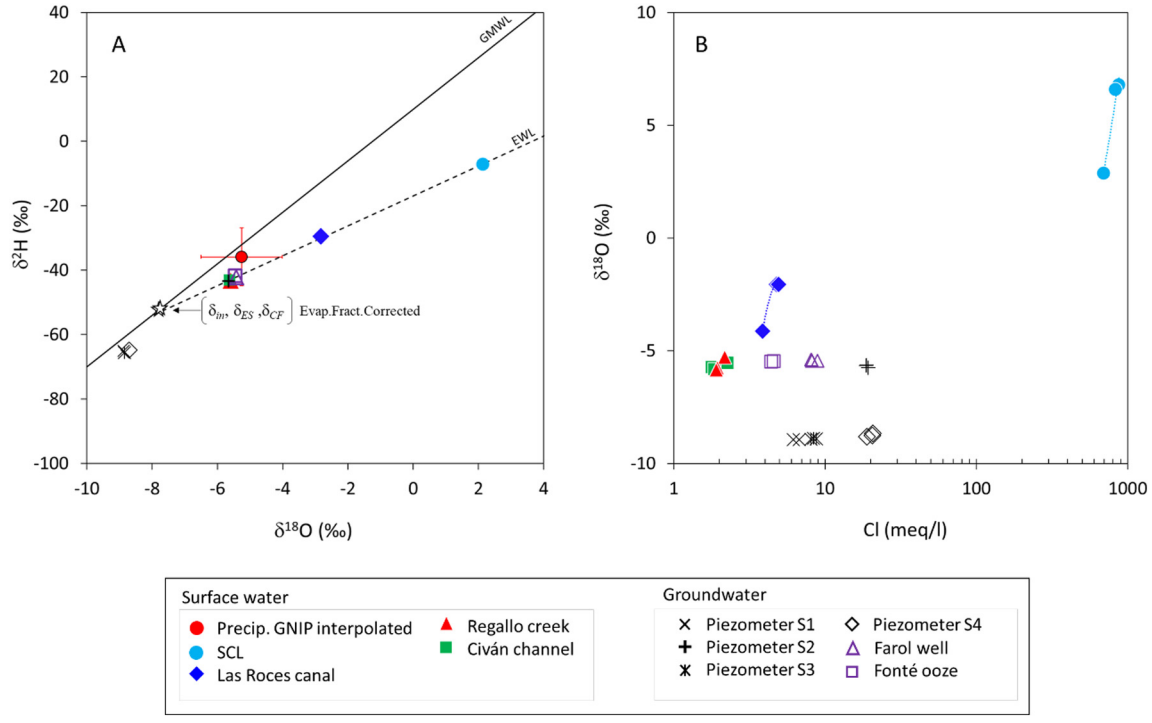

Fig. 13. (A) Average water isotopic composition at the different water sampling points. In the case of the GNIP-interpolated mean isotopic content (solid circle), the bars indicate the standard deviation. The star symbols correspond to the estimated δ_{ES}, δ_{CF} and δ_{in} values before being affected by evaporation fractionation. The GMWL is that of slope 8 and intercept 10‰. The depicted EWL is the regression line to the isotopic content of the surface water samples, showing a slope of 4.65. (B) Relationship between $\delta^{18}O$ and Cl in the analysed water samples.

The origin of recharge can be also analysed considering environmental tracers. ITGE (1992) provides the average isotopic content of precipitation measured at different points distributed along the Iberian Range. In this mountain range, the isotopic altitudinal line (IAL) of precipitation presents a slope ($\nabla_z\delta^{18}O_P$) of −0.38‰/100 m (Fig. 14). Looking at the isotopic content of groundwater from springs located both in the Iberian Range (ITGE, 1994) and in the contact between the carbonate aquifer and the Tertiary sediments of the Ebro Basin, it can be shown that these values plot on a line with a slope $\nabla_z\delta^{18}O_{GW}$ which is lower than $\nabla_z\delta^{18}O_P$. This is consistent with a sloping aquifer situation (Custodio and Jódar, 2016), in which recharge is favoured along the mountain slopes by the large outcroppings of high permeability Jurassic 'carnioles' and limestones of the Iberian Chain (Sánchez et al., 1999). The different waters represented in Fig. 14 have d values only slightly <10‰, indicating that there is at most a slight evaporation effect during rain fall through the air or in the top soil when vegetation is scarce. Therefore, correcting the plot for this effect will no modify significantly the figure.

The average isotopic content of groundwater found in the SCL is −8.8‰. This value is close to that of precipitation in the slopes of the Iberian Range. Moreover, $\nabla_z\delta^{18}O_P$ allows estimating the recharge elevation zone for groundwater in SCL, which is comprised between 1000 and 1700 m a.s.l. This result is coherent with the altitudes of the Iberian Range at the southern part of the study area, where large outcroppings of high permeability, karstified and fissured Jurassic 'carnioles' and limestones exist (Sánchez et al., 1999). The estimated recharge elevation interval has not been corrected by the slope effect, as expected changes would be small. Additionally, this origin of recharge is supported by the very low to nil tritium content reported by Gómez-Martos (1992) for groundwater.

5.2. Building the hydrogeological conceptual model for the SCL

The hydrogeological conceptual model (HCM) is the basis of the hydrogeological system analysis. It considers in a comprehended way all the flow terms driving the hydrogeological system response (Betancur et al., 2012). From the perspective of surface water inflows into the SCL, three sources with different isotopic fingerprint can be found: (1) direct precipitation over the lake (Q_P), (2) direct water transfer through the connection canal from Laguna de las Roces (Q_{CF}), which in turn receives water from the Civán Channel and the Regallo Creek, and (3) surface and interflow runoff generated by rainfall and irrigation returns flows (Q_{RF}). The SCL is located at the bottom of an endorheic basin. No surface water leaves the system nor does it seem possible under the most extreme high water level conditions. Therefore, the only plausible surface outflow is evaporation (Q_E). The lake water salinity shows a seasonal variation. The minimum is in spring, coinciding with the largest water inflow from irrigation return flows and precipitation and the maximum is produced in summer because the high evaporation rates driven by the high temperatures. Additionally, the lake water salinity presents a high annual variability (Fig. 10), with an average TDS value of 60 g/L for the period 1986–2016, although less than the values found in the neighbouring endorheic saline lakes abovementioned.

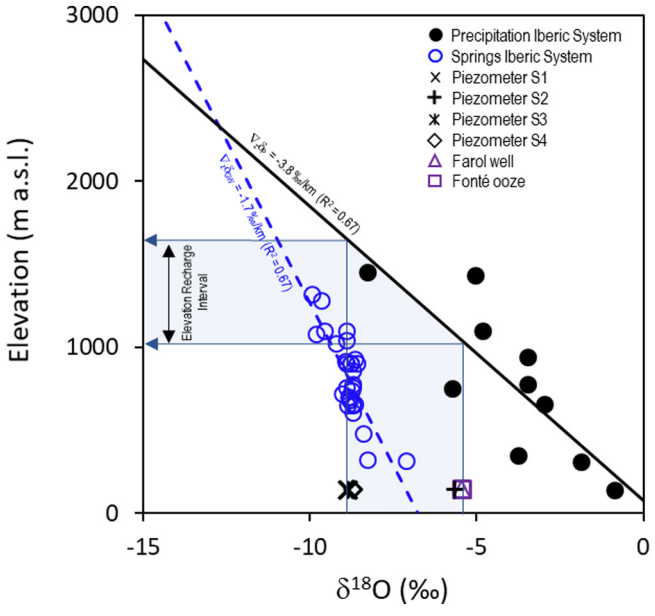

Fig. 14. Relationship between elevation and average isotopic content in precipitation (δ_P; solid circles) and in groundwater (δ_{GW}; empty circles), for the different sampling points (i.e. rain gauges and springs) along the Iberian Range, as reported in the literature (Table SM5 and Fig. SM13 - Suppl. Mat.). The solid and dashed lines correspond to the regression lines of elevation with δ_P and δ_{GW}. They represent the isotopic altitudinal lines (IALs) of precipitation and groundwater, respectively, for the Iberian Range.

The relatively small lake level variability and almost an order of magnitude salinity variation can be explained by the adequate combination of inflows and outflows. Nevertheless, this happens rarely under natural conditions. A more plausible mechanism is the existence of outflow thresholds in the sediments limiting the lake, corresponding to the buried paleochannels located at the NE of the SCL, as found during the geophysical characterization of the study area. These paleochannels drain the SCL when the lake level is above a certain threshold, allowing the outflow of the lake inflow excesses as groundwater discharge (Q_{GWO}) and thus giving stability to the SCL levels.

The hidden SCL draining mechanism is indeed activated because it prevents the lake water to become oversaturated in halite. Moreover, the long-term salt mass accumulation in a lake in which water only leaves the system by evaporation should be a monotonously increasing function that would drive the dissolved salt concentration up to saturation relative to the most soluble minerals (Carter, 1996). This is the situation observed in several salt lakes in the neighbouring of the SCL, such as El Saladar, La Playa and La Salineta lakes, where the sodium chloride concentration reaches 152, 154 and 250 g/L, respectively (Auqué et al., 1995; Valero-Garcés et al., 2000b, 2005). Nevertheless, a solid phase thick salt accumulation layer has not been found in the sediment cores drilled by Valero-Garcés et al. (2000a) during the limnological characterization of the SCL. This result is relevant considering that the SCL exists as a hydrologic system since at least the Late Pleistocene.

The relationship between the SCL and groundwater is not only limited to the lake outflows. As pointed out by the isotopic tracers, groundwater recharged in the slopes of the Iberian Range also feeds the SCL. Although Valero-Garcés et al. (2000a). De Wit et al. (2013) and De Wit (2016) did not evaluate the groundwater inflows into the SCL (Q_{GWI}), they assumed them as negligible.

According to all the available information, Fig. 15 presents the conceptual water balance model for the SCL.

For the water balance calculations it is assumed that the lake is in steady state, in coherence with the no trending surface water level observed (Fig. 6). Therefore, a long-term water balance is performed. However, the existing data are not enough to establish with confidence if there is in long-term steady state of salinity. As said before, the hypothesis of a current trend to dissolved salts dilution in the lake might be not null. No historical data on the SCL water isotopic composition is available. Thus, the steady state assumption is only a first approach to understand the system gross functioning, but this has to be reconsidered when further data will be available, especially time-series data.

Under the steady-state situation, the average or long-term total water inflow in the SCL (Q_{in}) is equal to the total water outflow (Q_{out}).

$$Q_{in} = Q_{out} \quad (1)$$

It is possible to evaluate the inflow contribution that represents the groundwater discharge to the total water inflow in the SCL if the other

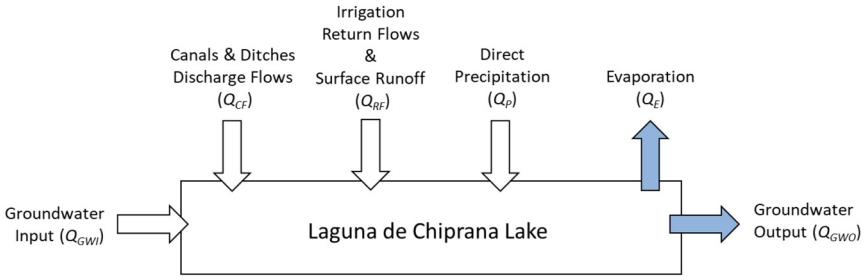

Fig. 15. Conceptual water balance model for the Salada de Chiprana Lake. White and blue shaded arrows stand for water inflows and outflows to the lake, respectively. (For interpretation of the references to colour in this figure legend, the reader is referred to the web version of this article.)

water balance terms and their corresponding isotopic content are known. Focussing on the inflow term of Eq. (1), the following equation system can be written:

$$Q_{in} = Q_P + Q_{CF} + Q_{RF} + Q_{GWI} \tag{2}$$

$$Q_{in}\delta_{in} = Q_P\delta_P + Q_{CF}\delta_{CF} + Q_{RF}\delta_{RF} + Q_{GWI}\delta_{GWI} \tag{3}$$

where δ_i [−] is the isotopic content of the i^{th} water balance term. The unknown variables of the above equation system are Q_{GWI} and Q_{in}. By rearranging terms, Q_{GWI} can be obtained as

$$Q_{GWI} = \frac{Q_P(\delta_{in}-\delta_P) + Q_{CF}(\delta_{in}-\delta_{CF}) + Q_{RF}(\delta_{in}-\delta_{RF})}{(\delta_{GWI}-\delta_{in})} \tag{4}$$

In these equations, Q is flow, δ is the isotopic composition, in is inflow, out is outflow, P is precipitation, CF is canal flow, RF is return irrigation flow, and GWI is groundwater inflow.

All the water flow variables included in the previous equations [i.e. Q_i, where the subscript i stands for the i^{th} water balance term] are expressed as flow rates [L^3T^{-1}]. Nevertheless, these variables can be also expressed in terms of water flows (i.e. volume of water per unit of area and unit time, with dimensions [LT^{-1}]), without loss of validity.

To estimate Q_{GWI} it is necessary to know previously the different water balance terms and the corresponding isotopic contents involved in Eq. (4). The mean values of Q_P, Q_{RF} and Q_{CF} are obtained from averaging the corresponding time series for the period 1994–2012. The respective values are 0.045, 0.081 and 0.079 hm^3/yr (DGA, 2012). The isotopic content terms of Eq. (4) are obtained by averaging the corresponding time series values measured during the field survey carried out for this work in 2016, so they do not represent an average situation but a temporal one. Therefore, results are only a first approach, as above stated.

Focussing on the outflow terms of Eq. (1) and considering that the SCL is located at the bottom of an endorheic basin from which water can only outflow by evaporation and transfer/recharge to the underlying aquifer, the outflow term of Eq. (1) can be written as

$$Q_{out} = Q_E + Q_{GWO} \tag{5}$$

where Q_E is evaporation on the lake surface, which is assumed to be equal to 1500 mm/yr (DGA, 2012), and Q_{GWO} is groundwater outflow (water that infiltrates through the lake bottom or leaks through the lake boundary).

To estimate the role played by groundwater (Q_{GWI}) in the input Water Mass Balance (WMB) (Eq. 4), it is necessary to characterize the mean values of the isotopic content of water from surface runoff (δ_{ES}), irrigation channels (δ_{CF}) and total water inflow into the SCL (δ_{in}). δ_{ES} is taken equal to the average value of the isotopic contents of Civán Channel and Regallo Creek, δ_{CF} equal to the mean isotopic content of water flowing through the Roces Canal, and δ_{in} equal to the mean isotopic content of the SCL. As δ_{ES}, δ_{CF} and δ_{in} are affected by isotopic fractionation due to evaporation, they cannot be used directly in Eq. 4. δ_{ES}, δ_{CF} and δ_{in} have to be estimated before the evaporation fractionating process affected them. In each case, the intersection of the GMWL with the corresponding EWL provides a first estimation of the original non-fractionated isotopic content value (Fig. 13). The salinity of Civán Channel, Regallo Creek, Fonté ooze, Farol well and S3 are original from regional recharge and not due to surface evaporation, as happens for S1, S3 and S4, but isotopically lighter. Only the water samples from the Roces Canal and SCL show isotopic evaporation effects, but data is too scarce to define the evaporation evolution.

Once δ_P, δ_{in}, δ_{ES} and δ_{GWI} have been obtained, the average values of Q_{GWI} and Q_{in} can be estimated by solving the equations Eqs. 2 and 3. The results are 0.503 and 0.064 hm^3/yr for Q_{in} and Q_{GWI}, respectively. The value for Q_{GWI} is $0.13Q_{in}$. These values depend on quite uncertain data. Therefore, the results have to be taken as a first approach.

In steady state, the total water inflow (Q_{in}) into the SCL equals the total water outflow (Q_{out}) from the SCL (Eq. 1). As the SCL is located at the bottom of an endorheic basin, water leaves the SCL only by evaporation (Q_E) and infiltration to recharge the aquifers (Q_{GWO}). Q_E equals to 0.3 hm^3/yr. Q_E can be also estimated by Eq. (5) in terms of Q_{out} and Q_E, obtaining 0.203 hm^3/yr. Q_{GWO} is 40% of the total water outflow from the SLC (Q_{out}), whereas the remaining 60% corresponds to Q_E. Table 4 shows the values of all the WMB terms considered in the conceptual water balance model for the SCL (Fig. 6), expressed in mm/yr relative to an average 20 ha of the SCL (DGA, 2012).

The diverse researchers and hydrologists that have studied the area consider both the groundwater inflows and evapo-concentration as the main water processes that modify salinity in the SCL. This can be checked by means of a solute balance in the lake, taking into account the different water and mass inflows and the possible dissolution and precipitation processes, with the help of a hydrochemical code. The scarce data available does not allow performing a dynamic balance. However, an approach is possible by assuming that the SCL is in long-term steady state and the average values of the variables are reasonably known. This is true for salinity, except for irrigation water and surface runoffs (Q_{RF}). It is not possible to reach the high concentration observed in the SCL by taking into account the weight of the different water source terms contributing to the SCL (Table 3) and assuming a hydrochemical composition for Q_{RF} similar to that measured in the Civán Chanel, Regallo Creek, and Roces Canal. It is not possible, even considering the hypothetic scenario in which the whole water inflow term Q_{in} estimated in the isotopic water balance would evaporate, thus increasing the lake water salinity by the corresponding evapo-concentration process. To explain the origin of the observed salinity in the SCL there are two plausible mechanisms, which are not mutually exclusive:

(1) the atmospheric deposition of airborne dust generated by strong local deflation processes (López et al., 1998; Gomes et al., 2003) and by the intense agricultural activities. The local strong wind transports dust particles from the cropping out Tertiary materials, which are later trapped when they fall or collide with the SCL water surface (Comín et al., 1992),

Table 4
Inflow and outflow terms of the water balance (Q_j) in the SCL. The inflow terms include water from precipitation (Q_P), irrigation channels (Q_{CF}), irritation return flows (Q_{RF}), groundwater inflow (Q_{GWI}) and total water inflow (Q_{in}), whereas the outflow terms include evaporation (Q_E), groundwater outflow (Q_{GWO}) and total water outflow (Q_{out}). The flows are given in average absolute values and per unit lake surface area.

	Inflows					Outflows		
	Q_P	Q_{CF}	Q_{RF}	Q_{GWI}	Q_{in}	Q_E	Q_{GWO}	Q_{out}
Q_j (mm/yr)	270	620	1304	319	2514	1500	1014	2514
Q_j/Q_{in} (−)	0.11	0.25	0.52	0.13	1.00	0.60	0.40	1.00

(2) salts deposited on the soils of the area and leached by rainfall runoff and irrigation return flows (Q_{RF}), partly incorporated to groundwater. There is a possible contribution from the Tertiary sediments (Comín and Forés, 1990), but their relevance is not known and is possibly small.

Estimating the hydrochemical composition of Q_{RF} while considering the effects of re-concentration by evaporation in the SCL, it is possible to explain the mean hydrochemical composition observed in the lake. Q_{RF} accounts for the 96.39% of the mean dissolved salts income into the SCL. Q_{CF}, Q_{GWI} and Q_P represent the 1.74%, 1.86% and 0.01%, respectively. These figures are the result of calculations with uncertain data, so they are a first approach. In any case, Q_{RF} is the key factor to explain the high salinity of the SCL.

The estimated groundwater discharge can be used to infer hydrogeological information about the Terciary materials through which groundwater flows. Darcy's Law (Eq. 6) quantifies water flow (q [LT^{-1}]) through a porous medium in terms of the saturated soil conductivity (K [LT^{-1}]) and the piezometric gradient (∇h [−])

$$q = -K \cdot \nabla h \tag{6}$$

Assuming that q and ∇h are known and equal to Q_{GWI} and $\nabla_z h$, respectively, Darcy's Law allows estimating the saturated hydraulic conductivity of the Tertiary materials through which groundwater flows. The K value is 3 mm/d, a low one that is consistent with that estimated through the geophysics soundings for the materials of the detritic Caspe Formation.

5.3. A step ahead toward the SCL management

Endorheic salt lakes are a common hydrologic feature in arid/semi-arid areas around the world, where regional evidences suggest a current net decline in endorheic water storage driven by global warming and especially by anthropogenic activities (Wurtsbaugh et al., 2017). In these zones, salt lakes are vulnerable to small flux variations, which are amplified by human activities such as inflow water diversions and groundwater pumping for agricultural purposes. Many iconic large salt lakes are severely affected already such as the Aral Sea (Micklin, 2010) or the Urmia Lake (Hassanzadeh et al., 2012) in Central Asia (Fig. 16), but also small endorheic salt lakes almost consisting in surface 'windows' of shallow water-tables are affected, therefore reducing their values as natural assets.

Changes in local hydrology may have large effects on endorheic saline lakes and their associated ecosystems. Given the fragility of these hydrological systems, and the lack or overlooking of a well-founded management plan, it is not surprising that many of these lakes have been gained (Goerner et al., 2009) and lost (Micklin, 1988, 2007) due to anthropogenic interference. In most cases, lacustrine ecosystems have been severely damaged as a result of large salinity variations driven by inadequate or absent managing processes.

A water budget supported by a robust HCM is critical to characterize the relative contributions of natural inflows variability and anthropogenic impacts to endorheic saline lakes. Conceptual models encourage science informed discussions on how preserving and maintaining saline lakes at fully functional levels. The development of such conceptual models is based on interpreting as a whole all the available hydro-

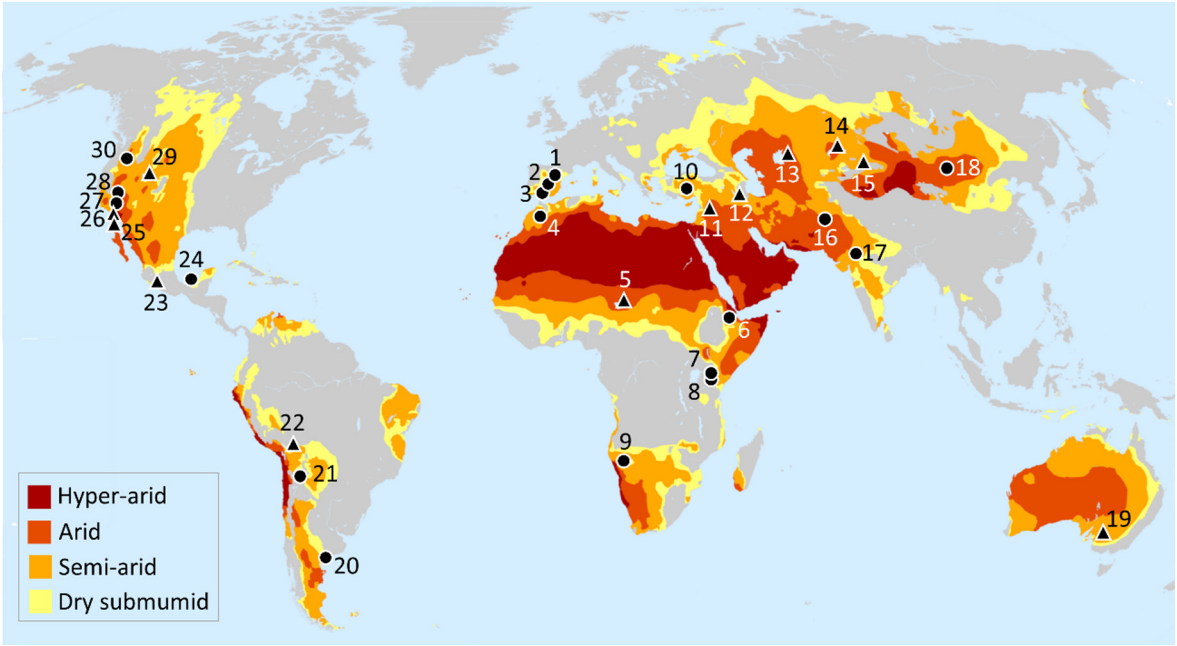

Fig. 16. Drylands of the world based on the aridity index (Berrahmouni et al., 2015), and location of some of the world's salt lakes impacted by water diversions and/or climate change. Triangles and circles indicate lakes with an initial unaffected surface area larger and lower than 250 km^2, respectively. Numbers correspond to the lake identification codes (Table SM6 - Suppl. Mat.).

geological information, including geological knowledge and monitoring data (Betancur et al., 2012).

In the SCL, the geological settings in the neighbouring of the lake fully condition the behaviour of the whole hydrogeological system. Despite of that, the hydrogeological characterization of this area is very scarce. The Tertiary materials in which the lake is located prevent to gain insights about the hydrogeological system at the local scale. To overcome this problem, the applied geophysical techniques have proven a successful approach. These techniques have shown how groundwater in the SCL area is associated with sandstone paleochannels that surround the lake. This is true even in the N-NE part of the lake, where the paleochannels are not evident since they are buried below a thin cover of quaternary sediments. The sandstone paleochannels are embedded in the low hydraulic conductivity (1 mm/d) Caspe Formation, which behaves as aquitard. This aquitard both feds and drains the sandstone paleochannels depending on the piezometric distribution around the SCL. The Caspe Formation rests on a marl and limestone formation, which is assumed hydraulically more continuous and transmissive.

The SCL is an unpaired permanent hypersaline lake in Western Europe that hosts rare and endangered microbial mats. The sediments accumulated in the SCL indicate that the lake became permanent coinciding with changes in both, climate and land use in the 17th century (Valero-Garcés et al., 2000a). Since then, the irrigation return flows into the SCL have been generating the conditions for maintaining the biological lake assets.

Algal mats have been present in the SCL since long time ago. Their presence was not interrupted by the hydrological changes after the 17th century and continues today when agriculture is using fertilizers at least since 50 years ago. The water balance shows that current conditions are dominantly anthropic. Then, the algal mats are the result of the existence of water in the lagoon, with a different hydrological regime, but with similar hydro- and bio-chemical circumstances. This can be explained by the fact that the origin of water both direct and after evapoconcentration in the agricultural and irrigation return flows, does not differ essentially from natural conditions, as local waters are applied. It can be assumed that dissolved nutrients in water from agricultural practices has at most a small effect as phosphates are trapped (co-precipitated) in the calcareous terrain. This helps in reducing the effect of the possible increase in nitrates. These are aspects that up to now seem not being studied, as well as the impact of pesticides, which could be retained in the soil and aquifer material.

To try to correct current problems in the SCL, nature-based solutions for environmental management have been proposed (Eggermont et al., 2015). This has opened the discussion on whether reestablishing the natural climatic and hydrological factors driving the hydrological behaviour of the SCL or promoting the conservation of specific bacterial communities and ecosystems. The former option will transform the SCL in one more among many other temporary saline lakes scattered in the Tertiary Ebro Basin (Ibáñez, 1975a, 1975b; Pueyo-Mur and Inglès-Urpinell, 1987; García-Vera, 1996), while eliminating the bacterial mats and impacting on the lake associated plankton (Alfonso et al., 2017) and macrobenthic communities (Alcocer et al., 1997). Moreover, this option will impact the whole ecological community of this highly valuable SCL ecosystem, because the lake serves as habitat and/or nesting centre for a number of endangered migrating waterfowls (De Juana and Garcia, 2015). The second option favors selecting and raising specific bacterial mats that are more interesting from the perspective of the SCL oddness and are the main reason why the lake is recognized by the Ramsar Convention.

After what has been studied here and commented above on the current anthropogenic conditions, management actions should be carefully designed to minimize changes at the time the best protection is achieved. This needs considering the inflow and outflow of groundwater, the hydrochemical changes in water type and the short- and long-time behaviour of nutrients and pesticides in the soils and the terrain.

There are many examples of endorheic saline lakes severely affected by human activities due to uncalibrated consequences of the actions done (Williams, 1996, 2002; Moore, 2016). Lessons learnt from these hydrological systems show that simplistic regulation of the lakes water may led to changes in the lake salinity that may destroy the singularity of the hydrological systems. To preserve the SCL bacterial mats in a water balance changing scenario, this work provides a conceptual model that allows managing both water inflows into the lake and the associated water salinity through the robust criterium of the binomial HCM-WMB.

More research is needed to characterize deeply the relevant regional hydrogeological processes in the study area. It would be useful for gaining process understanding and refining both the HCM and WMB. Moreover, more research is needed to confirm the effectiveness of the management measurements implemented by the SCL stakeholders. The applied managing measures may become a living example of adaptation for minimizing the impact of climate change on hypersaline lakes around the globe.

6. Conclusions

The recharge zone of groundwater discharging in the SCL is in the Iberian Range system, from 1000 to 1700 m a.s.l. This is consistent with the long transit time, reflected in the absence of seasonal variations in the isotopic content.

The dry deposition of windborne dust form Tertiary sediments may be a prominent process driving the mass salt incomes into the SCL. The high salinity of the SCL is controlled by both the discharge into the lake of the surface-subsurface runoff generated by rainfall and the irrigation return flows and groundwater outflows. This hinders the lake water salinity to reach over-saturation in halite, although it is saturated to oversaturated relative to calcite and dolomite and also to gypsum in some moments.

Groundwater heads in the SCL do not vary significantly in time, indicating the stability of groundwater discharge into the lake. The mean annual groundwater discharge relative to the SCL surface is 319 mm, corresponding to 13% of the total water inflow. Groundwater is not a dominant term in the SCL salinity balance, but it is relevant enough to be considered in the management of the ecological peculiarities of the area.

Groundwater outflow from the SCL is a key process that limits the lake water salinity. The binomial HCM-WBL provides a sharp tool to support the development of conservation measures for this athalassic hypersaline lake. Simplistic regulation of surface water may lead to changes that may destroy the singularity of the area.

CRediT authorship contribution statement

J. Jódar: Conceptualization, Data curation, Visualization, Formal analysis, Writing - original draft, Writing - review & editing.**F.M. Rubio:**Resources, Data curation, Writing - original draft, Writing - review & editing.**E. Custodio:**Formal analysis, Writing - original draft, Writing - review & editing.**S. Martos-Rosillo:**Writing - original draft, Writing - review & editing.**J. Pey:**Resources, Data curation, Writing - original draft, Writing - review & editing.**C. Herrera:**Writing - original draft, Writing - review & editing.**V. Turu:**Resources, Data curation, Writing - original draft, Writing - review & editing.**C. Pérez-Bielsa:**Resources, Data curation, Writing - original draft.**P. Ibarra:**Resources, Data curation.**L.J. Lambán:**Conceptualization, Funding acquisition, Project administration, Supervision, Writing - original draft, Writing - review & editing.

Declaration of competing interest

The authors declare that they have no known competing financial interests or personal relationships that could have appeared to influence the work reported in this paper.

Acknowledgments

This research was undertaken in the framework of the ZB51459 (2015) and ZB61539 (2016) contracts, funded by the Departamento de Desarrollo Rural y Sostenibilidad (Gobierno de Aragón, Spain), and the PIRAGUA project (EFA210/16/PIRAGUA) which is funded by the European Union through the Interreg-POCTEFA territorial cooperation program. The Spanish Agencia Estatal de Investigación (Spain) and the European Funds for Regional Development (European Union) are gratefully acknowledged for the financial support through CGL2015-68993-R project. The authors thank the Servicio Provincial de Agricultura, Ganadería y Medio Ambiente in Zaragoza (Gobierno de Aragón) for the sampling permits and the support of its technical staff.

We would also like to thank the anonymous reviewers for their constructive comments and suggestions which led to a substantial improvement of the paper.

Appendix A. Supplementary data

Supplementary data to this article can be found online at https://doi.org/10.1016/j.scitotenv.2020.138848.

References

AEMET/IM, 2011. Atlas Climático Ibérico–Iberian Climate Atlas. Agencia Española de Meteorología & IM. Madrid 1–80.

Alcalá, F.J., Custodio, E., 2008. Atmospheric chloride deposition in continental Spain. Hydrol. Process. 22, 3636–3650. https://doi.org/10.1002/hyp.6965.

Alcalá, F.J., Custodio, E., 2014. Spatial average recharge through atmospheric chloride mass balance and its uncertainty in continental Spain. Hydrol. Process. 28, 218–236. https://doi.org/10.1002/hyp.9556.

Alcalá, F.J., Custodio, E., 2015. Natural uncertainty of spatial average aquifer recharge through atmospheric chloride mass balance in continental Spain. J. Hydrol. 524, 642–661. https://doi.org/10.1016/j.jhydrol.2015.03.018.

Alcocer, J., Lugo, A., Escobar, E., Sánchez, M., 1997. The Macrobenthic Fauna of a Former Perennial and Now Episodically Filled Mexican Saline Lake. https://doi.org/10.1007/BF01997141.

Alfonso, M.B., Zunino, J., Piccolo, M.C., 2017. Impact of water input on plankton temporal dynamics from a managed shallow saline lake. Annales de Limnologie-International Journal of Limnology. vol. 53. EDP Sciences, pp. 391–400. https://doi.org/10.1051/limn/2017023.

Andrews, R.J., Barker, R., Heng, L.M., 1995. The application of electrical tomography in the study of the unsaturated zone in chalk at three sites in Cambridgeshire, United Kingdom. Hydrogeol. J. 3 (4), 17–31. https://doi.org/10.1007/s100400050055.

Araguás-Araguás, L., Froehlich, K., Rozanski, K., 2000. Deuterium and oxygen-18 isotope composition of precipitation and atmospheric moisture. Hydrol. Process. 14, 1341–1355. https://doi.org/10.1002/1099-1085(20000615)14:8<1341::AID-HYP983>3.0.CO;2-Z.

Auqué, L.F., Vallès, V., Zouggari, H., López, P.L., Bourrié, G., 1995. Geoquímica de las lagunas saladas de los Monegros (Zaragoza). l. Determinación experimental de los efectos del reequilibrio mirabilita-solución con la temperatura en un sistema natural [Geochemistry of the salty lagoons of Monegros (Zaragoza). l. Experimental determination of the effects of mirabilite rebalancing-solution with temperature in a natural system]. Estud. Geol. 51 (5–6), 243–257. https://doi.org/10.3989/egeol.95515-6299.

Berlanga Herranz, M., Palau, M., Guerrero, R., 2017. Functional stability and community dynamics during spring and autumn seasons over 3 years in Camargue microbial mats. Front. Microbiol. 8, 2619. https://doi.org/10.3389/fmicb.2017.02619.

Bernard, J., 2007. Instruments and field work to measure a magnetic resonance sounding. Bol. Geol. Min. 118 (3), 459–472.

Berrahmouni, N., Regato, P., Parfondry, M., 2015. Global guidelines for the restoration of degraded forests and landscapes in drylands: building resilience and benefiting livelihoods. Forestry Paper No. 175. Food And Agriculture Organization of the United Nations (FAO 2015), Rome, p. 149.

Betancur, T., Palacio, C.A., Escobar, J.F. 2012. Conceptual models in hydrogeology, methodology and results. In: Kazemi GA (ed) Hydrogeology—A Global Perspective. InTech, pp 203–222. (https://www.intechopen.com/books/hydrogeology-a-global-perspective. Last access 30 March 2020).

Carter, V., 1996. Wetland hydrology, water quality, and associated functions. National Water Summary on Wetland Resources, pp. 35–48.

Castañeda, C., García-Vera, M.A., 2008. Water balance in the playa-lakes of an arid environment, Monegros, NE Spain. Hydrogeol. J. 16, 87–102. https://doi.org/10.1007/s10040-007-0230-9.

Comín, F.A., Forés, E., 1990. Comprobación experimental de la importancia relativa de las vías superficial y subterránea de inundación en la liberación de sales de sedimentos desecados [Assessing the efficiency differences between surface and subsurface flooding processes for dissolving salts from previously dried sediments]. Scientia Gerundensis 16, 69–77.

Comín, F.A., Julià, R., Comín, P., 1992. Fluctuations, the key aspect for the ecological interpretation of saline lake ecosystems. Homage to Ramon Margalef: Why there Is Such Pleasure in Studying Nature. vol. 8, p. 127.

Custodio, E., Jódar, J., 2016. Simple solutions for steady-state diffuse recharge evaluation in sloping homogeneous unconfined aquifers by means of atmospheric tracers. J. Hydrol. https://doi.org/10.1016/j.jhydrol.2016.06.035.

Davis, B.A.S., 1994. Paleolimnology and Holocene Environmental Change From Endorheic Lakes in the Ebro Basin, North-East Spain. Ph. D. Dissertation, University of Newcastle Upon Tyne, UK: 1–317. (https://theses.ncl.ac.uk/jspui/handle/10443/642. Last access 30 March 2020).

De Juana, E., Garcia, E., 2015. The Birds of the Iberian Peninsula. Bloomsbury Publishing 978-1-4081-2480-2 (720pp).

De Wit, R., 2016. Lake La Salada de Chiprana (NE Spain), an example of an athalassic salt lake in a cultural landscape. Lake Sciences and Climate Change, 43–60 https://doi.org/10.5772/6443.

De Wit, R., Falcon, L.I., Charpy-Roubaud, C., 2005. Heterotrophic dinitrogen fixation (acetylene reduction) in phosphate-fertilised Microcoleus chthonoplastes microbial mat from the hypersaline inland lake 'la Salada de Chiprana'(NE Spain). Hydrobiologia 534 (1–3), 245–253. https://doi.org/10.1007/s10750-004-1569-8.

De Wit, R., Guerrero, M.C., Legaz, A., Jonkers, H.M., Blocier, L., Gumiaux, C., Gautret, P., 2013. Conservation of a permanent hypersaline lake: management options evaluated from decadal variability of Coleofasciculus chthonoplastes microbial mats. Aquat. Conserv. Mar. Freshwat. Ecosyst. 23 (4), 532–545. https://doi.org/10.1002/aqc.2319.

Des Marais, D.J., 2003. Biogeochemistry of hypersaline microbial mats illustrates the dynamics of modern microbial ecosystems and the early evolution of the biosphere. Biol. Bull. 204 (2), 160–167. https://doi.org/10.2307/1543552.

Descloitres, M., Ruiz, L., Sekhar, M., Legchenko, A., Braun, J., Mohan-Kumar, M.S., Subramanian, S., 2008. Characterization of seasonal local recharge using electrical resistivity tomography and magnetic resonance sounding. Hydrol Proc 22, 384–394. https://doi.org/10.1002/hyp.6608.

DGA, 1994. Estudio hidrológico-hidrogeológico de la cuenca endorreica de las Saladas de Chiprana [Hydrologic-hydrogeologic study of the endorheic basin of Las Saladas de Chiprana]. ESHYG SL & Diputación General de Aragón, Zaragoza, pp. 1–128.

DGA, 1997. Plan de ordenación de los Recursos Naturales del Complejo Lagunar de Las Saladas de Chiprana [Bases for the Management of the Natural Resources in the Wetland Complex of the Saladas of Chiprana]. EPTISA & Diputación General de Aragón, Zaragoza.

DGA, 2012. Estudio hidrológico y balance de agua de la Reserva Natural de las Saladas de Chiprana [Hydrological study and water budged in the Saladas de Chiprana Natural Reserve]. Zeta Amaltea & Diputación General de Aragón, Zaragoza.

DGA, 2017. Campañas geofísicas, hidrogeoquímicas e isotópicas para la definición de la cuenca subterránea de las Saladas de Chiprana [Geophysical, Hydrogeochemical and Isotopic Surveys for Defining the Underground Geometry of the Chiprana Salt Flats]. IGME & Diputación General de Aragón, Zaragoza.

Eggermont, H., Balian, E., Azevedo, J.M.N., Beumer, V., Brodin, T., Claudet, J., Fady, B., Grube, M., Keune, H., Lamarque, P., Reuter, K., Smith, M., van Ham, C., Weisser, W.W., Le Roux, X., 2015. Nature-based solutions: new influence for environmental management and research in Europe. GAIA-Ecological Perspectives for Science and Society 24 (4), 243–248. https://doi.org/10.14512/gaia.24.4.9.

Espinosa Martínez, S., Custodio, E., 2016. Estimación de la escorrentía superficial para el cálculo de la recarga a los acuíferos del macizo kárstico de los Ports de Beseit (Tarragona, España) combinando balance de agua en el suelo y análisis de hidrogramas de caudales [Surface runoff for recharge estimation to the aquifers of the Ports de Beseit karstic massif (Tarragona, Spain) by combining a soil water balance and flow hydrographs]. Estud. Geol. 72 (1), e045. https://doi.org/10.3989/egeol.42132.374.

Espinosa, S., Custodio, E.; Loaso, C. 2014. Estimación de la recarga media anual de acuíferos: aplicación a la Vall Baixa de l'Ebre [Estimation of average yearly aquifer recharge: Application to the Ebre Low Valley]. In J. Gómez–Hernández & J. Rodrigo–Ilarri (eds.), II Congreso Ibérico de las Aguas Subterráneas. Valencia. Ed. Universitat Politècnica de València: 285–301. ISBN: 978–84–9048–239–1.

García-Vera, M.A., 1996. Hidrogeología de zonas endorreicas en climas semiáridos. Aplicación a Los Monegros (Zaragoza y Huesca) [Hydrogeology of endorheic zones in semi-arid climates. Application to Los Monegros (Zaragoza and Huesca)]. Diputación General de Aragón, Zaragoza (297 pp).

GEODE. 2011. Plan de Cartografía Geológica Continua Digital 1:50000. Instituto Geológico y Minero de España [Digital Continuous Geological Mapping Plan 1:50000. Geological and Mining Institute of Spain], (http://info.igme.es/cartografiadigital/geologica/Geode.aspx. Last access 30 March 2020).

Goerner, A., Jolie, E., Gloaguen, R., 2009. Non-climatic growth of the saline Lake Beseka, main Ethiopian rift. J. Arid Environ. 73 (3), 287–295. https://doi.org/10.1016/j.jaridenv.2008.09.015.

Gomes, L., Arrue, J.L., Lopez, M.V., Sterk, G., Richard, D., Gracia, R., Sabre, M., Gaudichet, A., Frangi, J.P., 2003. Wind erosion in a semiarid agricultural area of Spain: the WELSONS project. Catena 52 (3–4), 235–256. https://doi.org/10.1016/S0341-8162(03)00016-X.

Gómez-Martos, M., 1992. Aplicación de las técnicas isotópicas al estudio de problemas hidrogeológicos (2' Fase: 1990–92) [Application of Isotopic Techniques to the Study of Hydrogeological Problems (2nd Phase, 1990–92)]. Instituto Tecnológico GeoMinero de España. Ministerio de Industria y Energía.

Guerrero, M.C., De Wit, R., 1992. Microbial mats in the inland saline lakes of Spain. Limnetica 8, 197–204.

Guerrero, M., Balsa, J., Pascual, M., Martínez, B., Montes, C., 1991. Limnological characterization of the Salada de Chiprana Lake (Zaragoza, Spain) and its phototrophic bacteria communities. Limnetica 7 (1), 83–96.

Guerrero, J., Gutiérrez, F., Galve, J.P., 2013. Large depressions, thickened terraces, and gravitational deformation in the Ebro River valley (Zaragoza area, NE Spain): evidence of glauberite and halite interstratal karstification. Geomorphology 196, 162–176. https://doi.org/10.1016/j.geomorph.2012.06.024.

Hassanzadeh, E., Zarghami, M., Hassanzadeh, Y., 2012. Determining the main factors in declining the Urmia Lake level by using system dynamics modeling. Water Resour. Manag. 26 (1), 129–145. https://doi.org/10.1007/s11269-011-9909-8.

Herbst, D.B., 2001. Gradients of salinity stress, environmental stability and water chemistry as a templet for defining habitat types and physiological strategies in inland salt waters. Saline Lakes. Springer, Dordrecht, pp. 209–219. https://doi.org/10.1007/978-94-017-2934-5_19.

Ibáñez, M.J., 1975a. El endorreísmo del sector central de la depresión del Ebro (Endorheic drainage in the central Ebro depression). Cuadernos de Investigación Geográfica 7, 35–48.

Ibáñez, M.J., 1975b. El endorreismo aragonés [Aragonese endorheism]. Cuadernos de Aragón n° 8–9. Institución Fernando el Católico-CSIC, Zaragoza, pp. 31–44.

Iniesto, M., Villalba, I., Buscalioni, A.D., Guerrero, M.C., López-Archilla, A.I., 2017. The effect of microbial mats. In: the decay of anurans with implications for understanding taphonomic processes in the fossil record. Sci. Rep. 7, 45160. https://doi.org/10.1038/srep45160.

ITGE, 1992. Aplicación de las técnicas isotópicas al estudio de problemas hidrogeológicos (2a fase 1990–92) [Application of Isotopic Techniques to the Study of Hydrogeological Problems (2nd Phase 1990–92)]. Instituto Tecnológico GeoMinero de España, Madrid.

ITGE, 1994. Estudio de las aguas minero-medicinales, minero-industriales, termales y de bebida envasadas en la Comunidad Autónoma de Aragón. Informe de síntesis. Tomo 1 [Study of Mineral-Medicinal, Mining-Industrial, Thermal and Bottled Drinking Waters in the Autonomous Community of Aragon. Synthesis Report. Vol. 1]. Secretaria General de la Energia y Recursos Minerales. Ministerio de Industria y Energía. Instituto Tecnológico GeoMinero de España, Madrid.

Jellison, R., Williams, W., Timms, B., Alcocer, J., Aladin, N., 2008. Salt lakes: values, threats and future. In: Polunin, N. (Ed.), Aquatic Ecosystems: Trends and Global Prospects. Cambridge University Press, pp. 94–110. https://doi.org/10.1017/CBO9780511751790.010.

Jonkers, H.M., Ludwig, R., De Wit, R., Pringault, O., Muyzer, G., Niemann, H., Finke, M., De Beer, D., 2003. Structural and functional analysis of a microbial mat ecosystem from a unique permanent hypersaline inland lake: 'La Salada de Chiprana' (NE Spain). FEMS Microbiol. Ecol. 44 (2), 175–189. https://doi.org/10.1016/S0168-6496(02)00464-6.

Kafri, U., Goldman, M., 2005. The use of the time domain electromagnetic method to delineate saline groundwater in granular and carbonate aquifers and to evaluate their porosity. J. Appl. Geophys. 57 (3), 167–178. https://doi.org/10.1016/j.jappgeo.2004.09.001.

Legchenko, A., Valla, P., 2002. A review of the basic principles for proton magnetic resonance sounding measurements. J. Appl. Geophys. 50, 3–19. https://doi.org/10.1016/S0926-9851(02)00127-1.

Legchenko, A., Baltassat, J.M., Beauce, A., Bernard, J., 2002. Nuclear magnetic resonance as a geophysical tool for hydrogeologists. J. Appl. Geophys. 50 (1–2), 21–46. https://doi.org/10.1016/S0926-9851(02)00128-3.

Loke, M.H., 2001. Rapid 2D and 3D Resistivity and IP Inversion Using the Least Squares Method—RES2DINV. See Manual 3.4. Available via DIALOG. (http://www.geoelectrical.com. Last access 30 March 2020).

López, M.V., Sabre, M., Gracia, R., Arrue, J.L., Gomes, L., 1998. Tillage effects on soil surface conditions and dust emission by wind erosion in semiarid Aragon (NE Spain). Soil Tillage Res. 45 (1–2), 91–105. https://doi.org/10.1016/S0167-1987(97)00066-4.

Lubczynski, M., Roy, J., 2003. Hydrogeological interpretation and potential of the new magnetic resonance sounding (MRS) method. J. Hydrol. 283 (1–4), 19–40. https://doi.org/10.1016/S0022-1694(03)00170-7.

Lubczynski, M.W., Roy, J., 2007. Use of MRS for hydrogeological system parameterization and modelling. Bol. Geol. Min. 118 (3), 509–530.

Mazáč, O., Kelly, W.E., Landa, I., 1985. A hydrogeophysical model for relations between electrical and hydraulic properties of aquifers. J. Hydrol. 79 (1–2), 1–19. https://doi.org/10.1016/0022-1694(85)90178-7.

Meadows, V.S., Reinhard, C.T., Arney, G.N., Parenteau, M.N., Schwieterman, E.W., Domagal-Goldman, S.D., Lincowski, A.P., Stapelfeldt, K.R., Rauer, H., Das-Sarma, S., Hegde, S., Narita, N., Deitrick, R., Lustig-Yaeger, J., Lyons, T.W., Siegler, N., Lee Grenfell, J., 2018. Exoplanet biosignatures: understanding oxygen as a biosignature in the context of its environment. Astrobiology 18 (6), 630–662. https://doi.org/10.1089/ast.2017.1727.

Micklin, P., 1988. Desiccation of the Aral Sea: a water management disaster in the Soviet Union. Science 241 (4870), 1170–1176. https://doi.org/10.1126/science.241.4870.1170.

Micklin, P., 2007. The Aral sea disaster. Annu. Rev. Earth Planet. Sci. 35 (1), 47–72. https://doi.org/10.1146/annurev.earth.35.031306.140120 2007.

Micklin, P., 2010. The past, present, and future Aral Sea. Lakes Reserv. Res. Manag. 15 (3), 193–213. https://doi.org/10.1111/j.1440-1770.2010.00437.x.

Moore, J.N., 2016. Recent desiccation of western Great Basin saline lakes: lessons from Lake Abert, Oregon, USA. Sci. Total Environ. 554, 142–154. https://doi.org/10.1016/j.scitotenv.2016.02.161.

Moreno, A., Sancho, C., Bartolomé, M., Oliva-Urcia, B., Delgado-Huertas, A., Estrela, M.J., Corell, D., López-Moreno, J.I., Cacho, I., 2014. Climate controls on rainfall isotopes and their effects on cave drip water and speleothem growth: the case of Molinos cave (Teruel, NE Spain). Clim. Dyn. 43 (1–2), 221–241. https://doi.org/10.1007/s00382-014-2140-6.

Muñoz-Jiménez, A., Casas-Sainz, A.M., 1997. The Rioja trough (N Spain): tectosedimentary evolution of a symmetric foreland basin. Basin Res. 9, 65–85. https://doi.org/10.1046/j.1365-2117.1997.00031.x.

Owen, R.J., Gwavava, O., Gwaze, P., 2006. Multi-electrode resistivity survey for groundwater exploration in the Harare greenstone belt, Zimbabwe. Hydrogeol. J. 14 (1–2), 244–252. https://doi.org/10.1007/s10040-004-0420-7.

Parkhurst, D.L., Appelo, C.A.J. 2013. Description of Input and Examples for PHREEQC Version 3—A Computer Program for Speciation, Batch-Reaction, One-Dimensional Transport, and Inverse Geochemical Calculations: U.S. Geological Survey Techniques and Methods, Book 6, Chap. A43: 1–497. (Available only at https://pubs.usgs.gov/tm/06/a43. Last access 30 March 2020).

Peel, M.C., Finlayson, B.L., McMahon, T.A., 2007. Updated world map of the Köppen–Geiger climate classification. Hydrol. Earth Syst. Sci. 11, 1633–1644. https://doi.org/10.5194/hess-11-1633-2007.

Plata, J.L., 1999. Técnicas convencionales de Geofísica de superficie aplicadas en hidrogeología. Actualidad de las técnicas geofísicas aplicadas en Hidrogeología (Conventional methods of surface applied geophysics in hydrogeology: current geophysical techniques applied in hydrogeology). University of Granada, Granada, pp. 21–32.

Plata, J.L., Rubio, F.M., 2007. Basic theory of the magnetic sounding resonance method. Bol. Geol. Min. 118 (3), 441–458.

Polerecky, L., Bachar, A., Schoon, R., Grinstein, M., Jørgensen, B.B., De Beer, D., Jonkers, H.M., 2007. Contribution of Chloroflexus respiration to oxygen cycling in a hypersaline microbial mat from Lake Chiprana, Spain. Environ. Microbiol. 9 (8), 2007–2024. https://doi.org/10.1111/j.1462-2920.2007.01317.x.

Pueyo-Mur, J.J., Inglès-Urpinell, M., 1987. Substrate mineralogy, pore brine composition, and diagenetic processes in the playa lakes of los Monegros and Bajo Aragón, Spain. In: Rodríguez-Clemente, R., Tardy, Y. (Eds.), Geochemistry and Mineral Formation in the Earth Surface. CSIC-CNRS, Granada, pp. 351–372.

Quirantes, J., 1971. Las calizas en el Terciario continental de Los Monegros (Limestones in the continental Tertiary of Los Monegros region). Estud. Geol. 27, 355–362.

Quirantes, J., 1978. Nota sobre las lagunas de Bujaraloz-Sástago [Technical note regarding the lagoons of Bujaraloz-Sástago]. Geographica 12, 30–34.

RAEMIA, 2019. Recarga natural a los acuíferos, metodología y soporte de la isotopía del agua. Aplicación a la planificación hidrológica y conocimiento de las aguas subterráneas en España (Natural aquifer recharge, methodology and support of water isotopes. Application to water planning and knowledge of groundwater in Spain). Prepared by E. Custodio, with the Review of J. Jódar and Contributions from J.V. Giráldez and A Sahuquillo, for UPC and SUEZ-CETAQUA. Technical University of Catalonia, Barcelona. ISBN: 978-84-9880-814-8 , pp. 1–1207. http://hdl.handle.net/2117/182282.

Ragon, M., Benzerara, K., Moreira, D., Tavera, R., López-García, P., 2014. 16S rDNA-based analysis reveals cosmopolitan occurrence but limited diversity of two cyanobacterial lineages with contrasted patterns of intracellular carbonate mineralization. Front. Microbiol. 5, 331. https://doi.org/10.3389/fmicb.2014.00331.

Rein, A., Hoffmann, R., Dietrich, P., 2004. Influence of natural time-dependent variations of electrical conductivity on DC resistivity measurements. J. Hydrol. 285 (1–4), 215–232. https://doi.org/10.1016/j.jhydrol.2003.08.015.

Rozanski, K., Araguás-Araguás, L., Gonfiantini, R., 1993. Isotopic patterns in modern global precipitation. Geophys. Monogr. Ser. 78, 1–36.

Rubin, Y., Hubbard, S.S. (Eds.), 2006. Hydrogeophysics, Water Science and Technology Library. vol. v. 50. Springer, Dordrecht, The Netherlands, pp. 1–523.

Rubio Sánchez-Aguililla, F.M., Ramiro-Camacho, A., Ibarra Torre, P., 2017. Métodos geofísicos en entornos naturales protegidos [Geophysical methods in protected environments. Electrical resistivity tomography]. Tomografía eléctrica. Bol. Geol. Min. 128 (1), 171–192 ISSN: 0366-0176. 10.21701/bolgeomin.128.1.010.

Ruiz, J.M., Rubio, F.M., Ibarra, P., García de Domingo, A., Heredia, J., Araguas, L. 2006. Contribución de la tomografía eléctrica en la caracterización del sistema hidrogeológico de la laguna de Fuente de Piedra (Málaga) [Contribution of Electrical Tomography to the Hydrogeological Characterization of the Laguna de Fuente de Piedra (Málaga) Hydrogeological System]. En: J.A. López-Geta, J.C. Rubio & G. Ramos (eds.), Las aguas Subterráneas en los Países Mediterráneos, 1: 353-358. IGME, Serie: Hidrogeología y Aguas Subterráneas 17. Madrid, España. ISBN: 84–7840-631-X.

Salvany, J.M., García-Veigas, J., Ortí, F., 2007. Glauberite-halite association of the Zaragoza gypsum formation (Lower Miocene, Ebro Basin, NE Spain). Sedimentology 54, 443–467. https://doi.org/10.1111/j.1365-3091.2006.00844.x.

Samper, J., Custodio, E., García Vera, M.A., 1993. Preliminary isotopic study of groundwater salinity variations in the closed–basin semiarid area of Los Monegros, Spain. Isotope Techniques in the Study of Past and Current Environmental Changes in the Hydrosphere and the Atmosphere. Intern. Atomic Energy Agency, Vienna, pp. 213–228 IAEA–SM–329/32.

Sánchez, J.A., Coloma, P., Pérez, A., 1999. Sedimentary processes related to the groundwater flows from the Mesozoic carbonate aquifer of the Iberian chain in the tertiary Ebro Basin, Northeast Spain. Sediment. Geol. 129 (3–4), 201–213. https://doi.org/10.1016/S0037-0738(99)00016-0.

Valero-Garcés, B.L., Navas, A., Machin, J., Stevenson, T., Davis, B., 2000a. Responses of a saline lake ecosystem in a semiarid region to irrigation and climate variability: the history of Salada Chiprana, Central Ebro Basin, Spain. Ambio, 344–350. http://www.jstor.org/stable/4315051.

Valero-Garcés, B.L., Delgado-Huertas, A., Navas, A., Machín, J., González Sampériz, P., Kelts, K., 2000b. Quaternary palaeohydrological evolution of a playa lake: Salada Mediana, Central Ebro Basin, Spain. Sedimentology 47 (6), 1135–1156. https://doi.org/10.1046/j.1365-3091.2000.00346.x.

Valero-Garcés, B.L., Navas, A., Machin, González Sampériz, P., Moreno-Caballud, A., Delgado Huertas, A., Stevenson, T., Davis, B., 2005. Lacustrine records of climate and environmental change in the Ebro Basin. Field Trip Guide-B2. Sixth International Conference on Geomorphology.

Valero-Garcés, B.L., Barreiro-Lostres, F., Errea, P., 2018. Bathymetric study and digital elevation model of the Laguna Salada de Chiprana (Zaragoza) [Estudio batimétrico y modelo digital del terreno de la Laguna Salada de Chiprana (Zaragoza)]. Instituto Pirenaico de Ecología.

Vidondo, B., Martinez, B., Montes, C., Guerrero, M.C., 1993. Physico-chemical characteristics of a permanent Spanish hypersaline lake: La Salada de Chiprana (NE Spain). Hydrobiologia 267 (1–3), 113–125. https://doi.org/10.1007/BF00018794.

Vouillamoz, J.M., Baltassat, J.M., Girard, J.F., Plata, J., Legchenko, A., 2007. Hydrogeological experience in the use of MRS. Bol. Geol. Min. 118 (3), 531–550.

Williams, W.D., 1996. What future for saline lakes? Environ. Sci. Policy Sustain. Dev. 38 (9), 12–39. https://doi.org/10.1080/00139157.1996.9930999.

Williams, W.D., 2002. Environmental threats to salt lakes and the likely status of inland saline ecosystems in 2025. Environ. Conserv. 29, 154–167. https://doi.org/10.1017/S0376892902000103 2002.

Wurtsbaugh, W.A., Miller, C., Null, S.E., DeRose, R.J., Wilcock, P., Hahnenberger, M., Howe, F., Moore, J., 2017. Decline of the world's saline lakes. Nat. Geosci. 10 (2017), 816–821. https://doi.org/10.1038/ngeo3052.

Yaramanci, U., Hertrich, M., 2007. Inversion of magnetic resonance sounding data. Bol. Geol. Min. 118 (3), 473–488.